LAWRENCE
LIVERMORE
NATIONAL
LABORATORY

LLNL-TR-420245

Aging Studies of Filled and Unfilled VCE

S. Letant, J. Herberg, C. Alviso, W. Small, H. Mulcahy, M. Pearson, T. Wilson, S. Chinn, R. Maxwell

November 13, 2009

Disclaimer

This work performed under the auspices of the U.S. Department of Energy by Lawrence Livermore National Laboratory under Contract DE-AC52-07NA27344.

Aging Studies of Filled and Unfilled VCE

Sonia E. Létant, Julie L. Herberg, Cynthia T. Alviso, Ward Small IV, Heather A. Mulcahy, Mark Pearson, Thomas S. Wilson, Sarah C. Chinn, and Robert S. Maxwell

Abstract

This report presents data on the effects of temperature and gamma radiation on the chemical and structural properties of both filled and unfilled VCE material produced by the Kansas City Plant using WR-qualified processes. Thermal effects up to 300 ºC and gamma irradiation doses of 1 MRad and 25 MRad were investigated under atmospheric conditions. Characterization techniques used in the study comprise Thermogravimetric Analysis (TGA), Differential Scanning Calorimetry (DSC), X-ray Diffraction (XRD), Tensile Testing, Solid Phase MicroExtraction – Gas Chromatography/Mass Spectrometry (SPME-GC/MS), phenol extraction followed by HPLC, and various Nuclear Magnetic Resonance (NMR) techniques including: ^{13}C, ^{13}C $\{^{1}H\}$ cross polarization (CP), ^{1}H magic angle spinning (MAS), $^{13}C\{^{1}H\}$ Wide-line-Separation (2D-WISE) and development of Center band-Only Detection of Exchange (CODEX).

Table of Contents

1. Introduction

VCE is an ethylene/vinyl acetate/vinyl alcohol terpolymer binder for filled elastomers (Figure 1) which is designed to accept high filler loadings in rubber compounds. Filled elastomer parts consist of the binder (VCE), a curing agent (Hylene MP, diphenyl-4,4'-methylenebis(phenylcarbamate)), a processing aid (LS, lithium stearate), and filler particles (typically 70% fraction by weight). The curing of the filled elastomer parts occurs from the heat activated reaction between the hydroxyl groups of VCE with the Hylene MP curing agent, resulting in a cross-linked network (Figure 2). The final vinyl acetate content is between 34.9 and 37.9%, while the vinyl alcohol content is between 1.27 and 1.78%.

Material characterization and aging studies had been performed on previous formulations of the VCE material [1-2] but the Ethylene Vinyl Acetate (EVA) starting copolymer is no longer commercially available. New formulations with replacement EVA materials are currently being established and will require characterization as well as updated aging models [3, 4].

This report presents data on the effects of temperature and gamma radiation on the chemical and structural properties of both filled and unfilled VCE material synthesized, milled, molded and cured at the Kansas City Plant using WR-qualified processes (see KCP-613-6051).

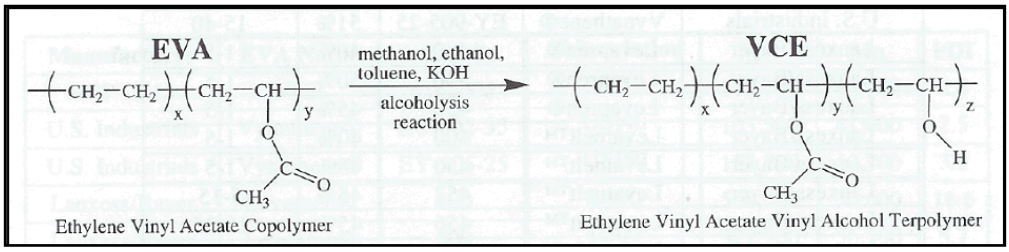

Figure 1: Base catalyzed alcoholysis reaction of EVA copolymer yielding VCE [3]. Typical VCE composition is 34.9-37.9% vinyl acetate, and 1.27-1.78% hydroxyl.

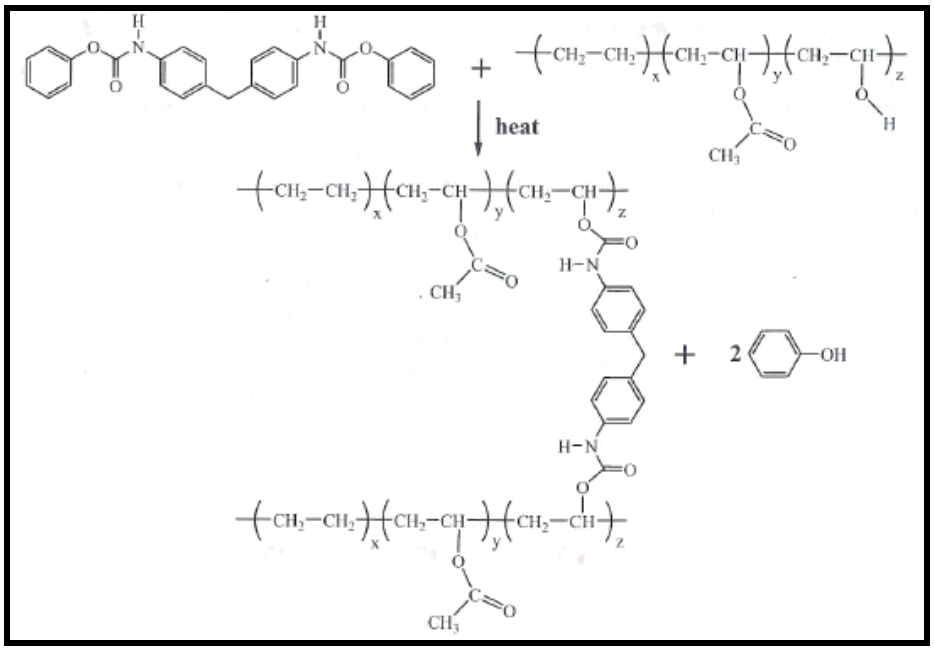

Figure 2: Curing reaction between VCE and Hylene MP[3].

2. Experimental Approach

Two sets of three VCE sheets (diameter: 11", thickness: 0.030") were synthesized, milled, molded and cured at the Kansas City Plant. The first set was processed with Hylene MP and LS only (unfilled VCE) and the second set was processed with Hylene MP, LS and WR filler (filled VCE). Parts were checked for uniformity using X-ray radiography and packaged with desiccant and heat-sealed sleeves prior to shipping.

For the gamma irradiation study, filled and unfilled samples were sealed with air into a plastic bag, placed into a stainless steel vessel, exposed to a 1.2 MeV, 5 kGray/hour, ^{60}C source and irradiated to 10 kGray (1 MRad) and 250 kGray (25 MRad) respectively. For the thermal aging study, unfilled samples were placed in a muffle furnace with air circulation for 12 hrs at 50, 100, 125, 150, 175, 200, 250 and 300 ºC respectively.

Characterization techniques used in the study comprise Thermogravimetric Analysis (TGA), Differential Scanning Calorimetry (DSC), X-ray Diffraction (XRD), Solid Phase MicroExtraction – Gas Chromatography/Mass Spectrometry (SPME-GC/MS), phenol extraction followed by HPLC and various Nuclear Magnetic Resonance (NMR) techniques including: ^{13}C, ^{13}C $\{^{1}H\}$ cross polarization (CP), ^{1}H magic angle spinning (MAS), $^{13}C\{^{1}H\}$ Wide-line-Separation (2D-WISE), and development of Center band-Only Detection of Exchange (CODEX). We also probed the stiffness of the VCE material through T_2 (spin-spin) relaxation NMR measurements.

3. Results and Discussion

Potential sources of chemical or structural degradation and their effects need to be identified prior to using VCE as a binder in engineering applications, particularly in enduring systems. Typical sources of degradation addressed in this report are isolated or combined exposures to oxygen, high temperatures, and gamma radiation. Such exposures have been reported to cause chemical modifications (production of volatile degradation products, incorporation of oxygen) as well as structural modifications (main chain scission, cross-linking, end-linking) in polymer materials.

Recent publications showed that ethylene vinyl alcohol (EVOH) copolymers were affected by electron and gamma radiation. EVOH was shown to scavenge oxygen in the presence of electron or gamma irradiation (electrons create radicals, which allows oxygen to react with the polymer to form aldehydes and ketones) [5]. In addition, the material was shown to be less crystalline [5], and more cross-linked [6] after irradiation. Reported effects of electron and gamma radiation on EVA copolymers also include oxygen incorporation and increased cross-linking [7,8].

To the best of our knowledge, there is no published data to date on the degradation of VCE terpolymers.

3.1. Radiation-induced degradation of VCE

Filled and unfilled VCE samples were gamma-irradiated with doses of 0, 1 and 25 MRad. Upon irradiation in air, the sample's appearance changed from clear to dark yellow (3). UV-vis absorption spectroscopy was performed on unfilled samples in order to spectrally characterize the absorption change (4). At high irradiation doses, a spectral feature appeared between 350 and 400 nm (a more pronounced peak was observed upon thermal aging, as may be seen on Figure

22), which may be attributed to the formation of polyconjugated bonds $(C=C)_n$, also called polynenes, upon gamma irradiation. The formation of polyenes is also attributed to the deacetylation of the vinyl acetate groups, which generates acetic acid (SPME-GS-MS showed a direct correlation between the acetic acid release and the gamma irradiation dose). Other potential sources of discoloration in VCE are large decomposition products of the Hylene MP cross-linking agent. While mono-substituted benzene rings such as phenol display absorption bands typically below 280 nm, di-substituted benzene rings typically display absorption bands between 280 and 380 nm.

At the exception of this change in color, samples remained identical in their macroscopic appearance (no noticeable changes in size, texture or surface appearance).

Figure 5 shows the surface of a pristine, filled VCE sample. Two size distributions of filler particles may be observed: larger sizes, in the 10 μm range, and smaller sizes, in the 1 μm range.

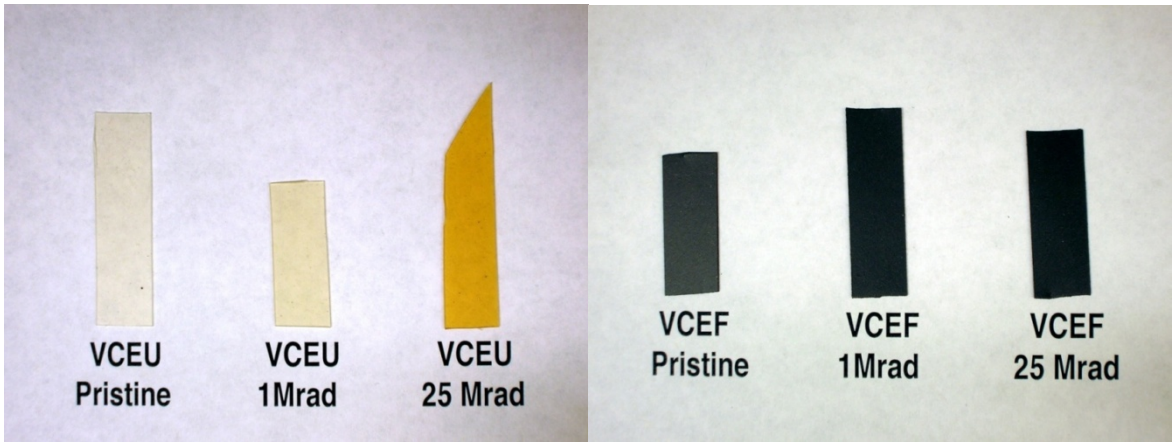

Figure 3: Photograph of unfilled (left) and filled (right) VCE samples after exposure to gamma radiation doses of 0, 1 and 25 MRad respectively.

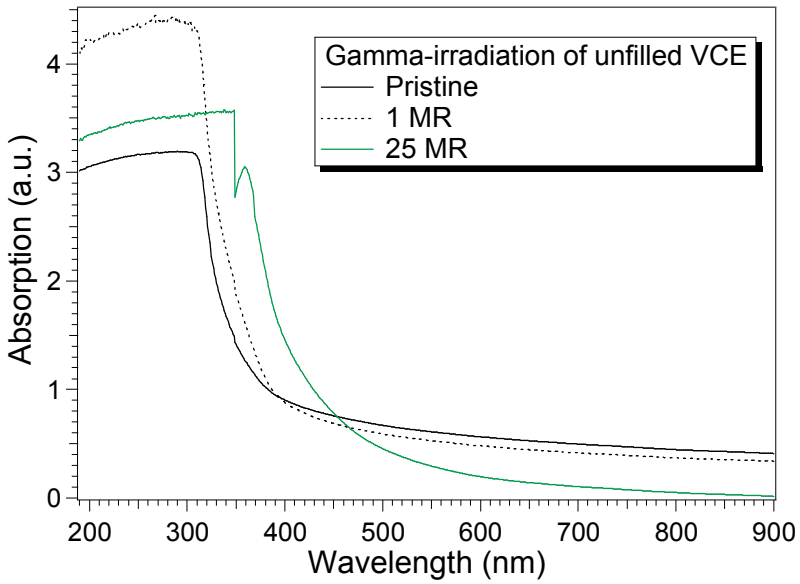

Figure 4: UV-vis absorption spectra of unfilled VCE samples after exposure to gamma radiation doses of 0, 1 and 25 MRad respectively.

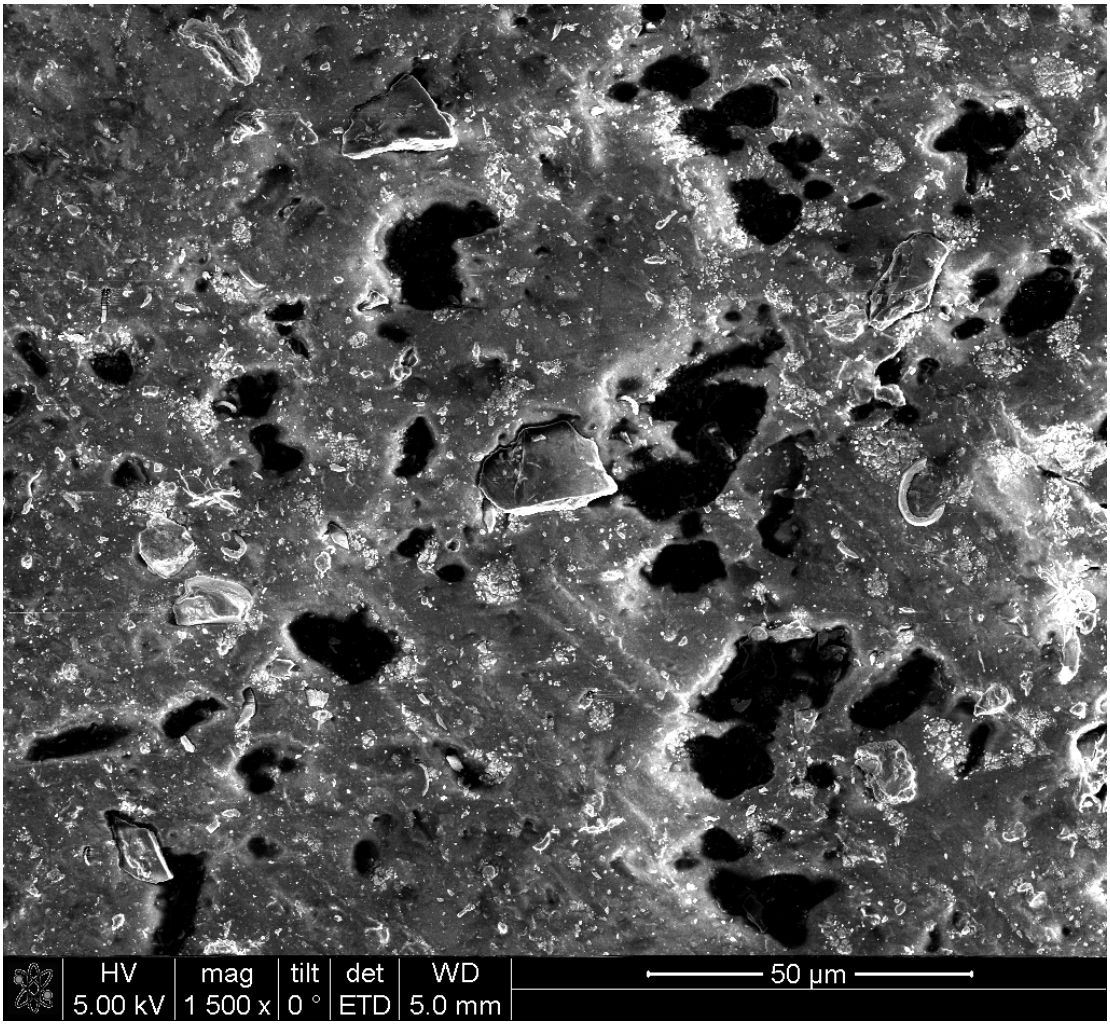

Figure 5: SEM image of a pristine, filled VCE sample.

3.1.1. Structural effects

3.1.1.1. Differential Scanning Calorimetry (DSC)

DSC experiments were performed using a Perkin Elmer Pyris Diamond instrument, under a flow of nitrogen gas of 20 mL/min. Sample discs were cut using a 2.5 mm diameter biopsy punch and individual discs were placed into aluminum pans, weighed, and submitted to the following temperature cycle: 2 min at 25 ºC, 25 to 200 ºC at 10 ºC/min, 2 min at 200 ºC, 200 to -60 ºC at 10 ºC/min, 10 min at -60 ºC, and -60 to 200 ºC at 10 ºC/min. Thermograms were base line-corrected to remove the contribution from the aluminum pans.

Heat flow versus temperature curves for the unfilled and filled VCE materials are shown in Figures 6 and 7 respectively, where each curve represents the average of two replicate samples. Thermograms show multiple and complex thermal behavior for the VCE terpolymer (one Tg and two peaks), due to the complex chain structure consisting of three monomers with varying sequence distribution as well as cross-links and pendent methylene bis(phenylcarbamate). Looking at the upper (heating) curves, the lowest temperature step is believed to be due to the glass transition of vinylacetate rich sequences. The sharp peak on the first heating curve at

approximately 40-42 ºC is commonly seen on first heating through a transition and may be due to the so-called "enthalpy relaxation" related to volume relaxation, to crystallization of shorter ethylene sequences, or even possibly to molecular associations of the aromatic cross-linker. There is literature evidence to suggest it is most likely due to crystallization of the shorter ethylene sequences [10]. Assignment of the third peak is also somewhat ambiguous – while literature [9] suggests this could correspond to crystallization of the longer ethylene sequences, other evidence strongly contradicts this. Both the absence of significant crystallinity from WAXS data (shown later) and the fact that the peak extends to temperatures too high to be related to ethylene crystallization indicate it must be something else. One possibility is that it is related to a phase transition from a multiphase to single phase morphology. Elucidating the exact mechanism will be the subject of future work.

Table 1 summarizes the data for both filled and unfilled samples in terms of enthalpy of fusion and heat capacity. The data shows no noticeable effects of gamma irradiation, indicating stable mobility, uniformity, cross-linking and crystallinity in the samples.

The addition of filler particles in the VCE matrix at a level of 70% by weight decreases both enthalpy of fusion and heat capacity. The decrease in the enthalpy of fusion from 5.7 to 1.2 J/g is explained by the reduced elastomer content in the material. The addition of filler particles also broadened transitions, as can be seen in Figure 7, which typically indicates less uniformity in the material as well as a higher level of cross-linking.

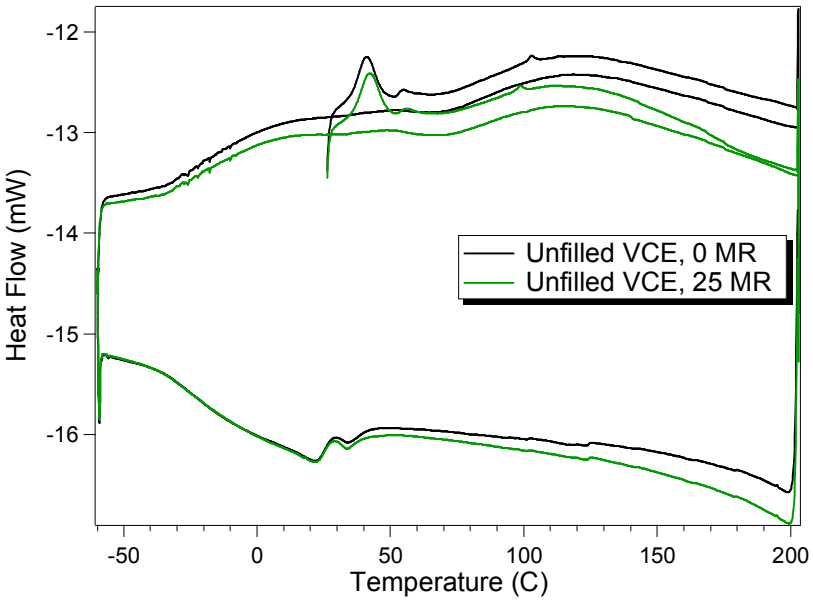

Figure 6: DSC curves for pristine and 25 MRad-irradiated unfilled VCE samples. Each curve represents the average of two replicate samples

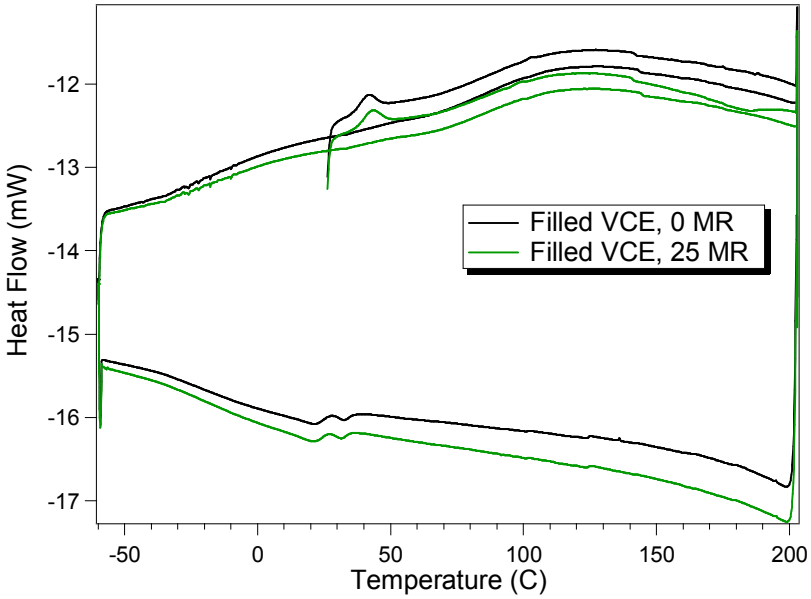

Figure 7: DSC curves for pristine and 25 MRad-irradiated filled VCE samples. Each curve represents the average of two replicate samples

Table 1. Quantitative summary of DSC experiments, comparing properties of pristine and gamma-irradiated VCE for both filled and unfilled samples.

Sample	Weight (mg)	Peak Location (°C)	Peak Area (mJ)	ΔH (J/g)	T_g (°C)	ΔC_p (J/g-°C)
VCE (Unfilled) 0 MR	3.5	40.9	21.5	6.2	-14.8	0.81
VCE (Unfilled) 0 MR	3.7	41.0	20.7	5.6	-14.8	0.71
VCE (Unfilled) 0 MR av.				**5.9**		**0.76**
VCE (Unfilled) 1 MR	3.6	40.5	20.7	5.7	-13.3	0.92
VCE (Unfilled) 1 MR	3.6	40.8	20.8	5.8	-15.8	0.90
VCE (Unfilled) 1 MR av.				**5.7**		**0.91**
VCE (Unfilled) 25 MR	3.8	42.7	21.4	5.6	-14.8	0.84
VCE (Unfilled) 25 MR	3.8	42.2	21.2	5.6	-12.7	0.79
VCE (Unfilled) 25 MR av.				**5.6**		**0.81**
VCE (Filled) 0 MR	6.7	41.5	7.6	1.1	-14.2	0.27
VCE (Filled) 0 MR	6.4	41.5	7.7	1.2	-12.9	0.30
VCE (Filled) 0 MR av.				**1.1**		**0.28**
VCE (Filled) 1 MR	6.7	41.4	7.1	1.1	-14.8	0.26
VCE (Filled) 1 MR	6.5	41.7	8.1	1.2	-15.2	0.28
VCE (Filled) 1 MR av.				**1.1**		**0.27**
VCE (Filled) 25 MR	6.4	42.7	8.8	1.4	-15.0	0.27
VCE (Filled) 25 MR	6.6	43.0	8.7	1.3	-12.7	0.26
VCE (Filled) 25 MR av.				**1.3**		**0.26**

3.1.1.2. X-Ray Diffraction (XRD)

XRD experiments were conducted on both pristine and irradiated unfilled VCE samples using a Philips vertical goniometer with Copper Ka radiation. Step scans from 20 to 80° (2θ) with step sizes of 0.02° were used, with a total acquisition time of 4 s.

As may be been on Figure 8, XRD did not detect any crystallinity in the samples, which indicates that the crystalline fraction (if any) is below the limit of detection of XRD (typically 5%).

Rough estimates of the crytallinity percentages calculated from the experimental values of the enthalpies of fusion presented in Table 1 (5.7 J/g for unfilled VCE, and 1.2 J/g for filled VCE) are 2 % for unfilled VCE and 0.4 % for filled VCE (Table 2) respectively. Such low crystallinity percentages should be expected in VCE terpolymers since the acetate content in these materials is significant (≥34.9 %). The bulky acetate groups are excluded from the polyethylene crystal lattice, which decreases the fraction of crystallizable units as the vinyl acetate content increases [11].

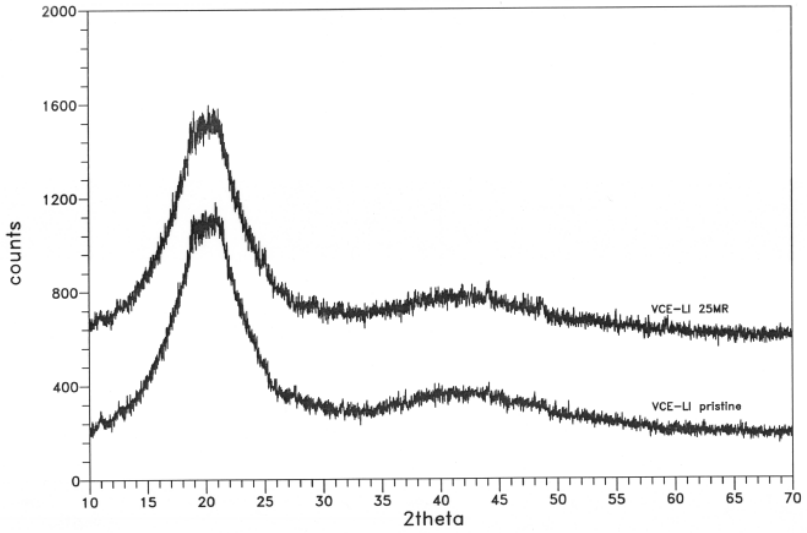

Figure 8: XRD spectra of pristine and 25 MRad-irradiated unfilled VCE samples acquired at room temperature.

Table 2. Estimate of crystallinity percentages in filled and unfilled VCE based on DSC results.

Sample	T_m (°C)	Peak area (mJ)	ΔH_f (J/g)	Crystallinity[1] (%)
Unfilled VCE	41	21	5.7	**2.0**
Filled VCE	42	8	1.2	**0.4**

[1] % crystallinity = (ΔHf / ΔHf*) x 100

ΔHf* = 285.8 J/g for PolyEthylene (Heat of fusion for 100% crystalline sample)[12]

3.1.1.3. Nuclear Magnetic Resonance (NMR)

The wideline separation (WISE) and Center band-Only Detection of Exchange (CODEX) NMR experiments were performed with a 7 mm DOTY NMR probe and the spinning speed for these experiments was 6 kHz.

To understand the effects of radiation on VCE, we performed $^{13}C\{^{1}H\}$ WISE NMR [13], which is typically used to explore the dynamics of polymers and blends through proton line shapes that are correlated with the carbon chemical shift. This data, shown in Figure 9, indicates that the VCE terpolymer dynamics does not significantly change, which confirms that this material is robust to gamma radiation.

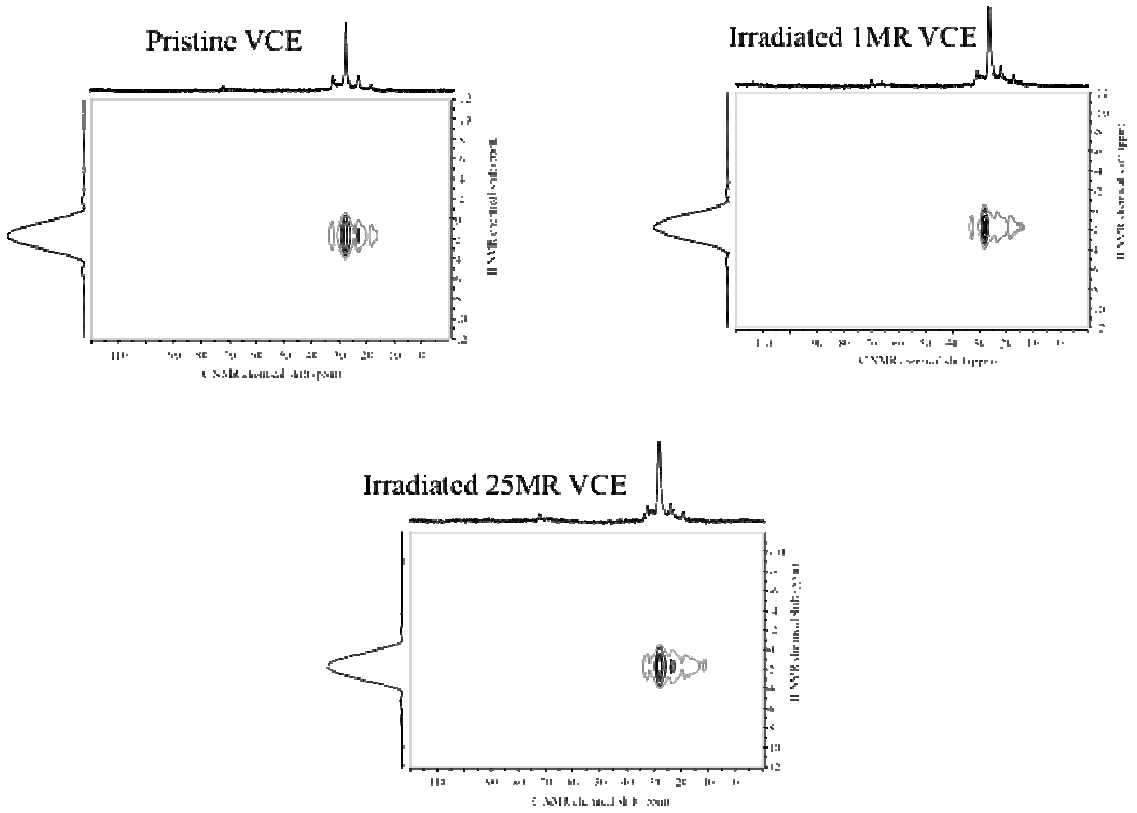

Figure 9: $^{13}C\{1H\}$ CPMAS 2D wide-line separation (WISE) NMR correlating ^{13}C chemical shifts with hydrogen mobility by observing the corresponding ^{1}H line widths and line shapes in unfilled pristine, 1 MRad, and 25 MRad-irradiated VCE samples.

To confirm the absence of changes in mobility and stiffness of the VCE polymer upon exposure to gamma radiation, we performed spin-spin relaxation (T_2-relaxation) NMR experiments on filled and unfilled pristine and 25 MRad-irradiated VCE. T_2 relaxation is inversely correlated to the relative stiffness of the bulk material. The data, presented in Figure 10, showed a double exponential, with a short and a long component. The long and short T_2 relaxation components showed a slight decrease in stiffness with a 25 MRad irradiation for the unfilled VCE and a slight increase in stiffness with a 25 MRad irradiation for the filled VCE. Overall, the T_2 experiments showed no significant changes in mobility or stiffness of the material upon gamma irradiation up to 25 MRad.

To further understand radiation effects on the VCE material, variable contact time array experiments were performed to determine the proton-carbon time constant, T_{CH}, and the proton spin-lattice time in the rotating frame, $T_{1\rho}$. ^{1}H-^{13}C cross polarization contact time (T_{CH}) depends on the dipolar coupling between the proton and carbon nuclei, and has shown a correlation to mechanical properties of the materials [14-16]. $T_{1\rho}$ reflects the long range proton-proton interactions. Figure 11 is a plot of the signal intensity as a result of a CP contact time array showing the CP buildup, which occurs at a rate of $1/T_{CH}$, and the CP decay, which occurs at a rate of $1/T_{1\rho}$ for all three samples. Table 3 summarizes the values of these time constants for pristine and gamma-irradiated VCE samples. A rigid polymer typically has a short T_{CH} and a long $T_{1\rho}$ [17–19]. In these experiments, $T_{1\rho}$ is effectively the same for all the samples, which

indicates that the backbone structure of the VCE material is robust. The fact that T_{CH} decreases with irradiation indicates a slight decrease in motion in the irradiated sample, which indicates a slight hardening of the material.

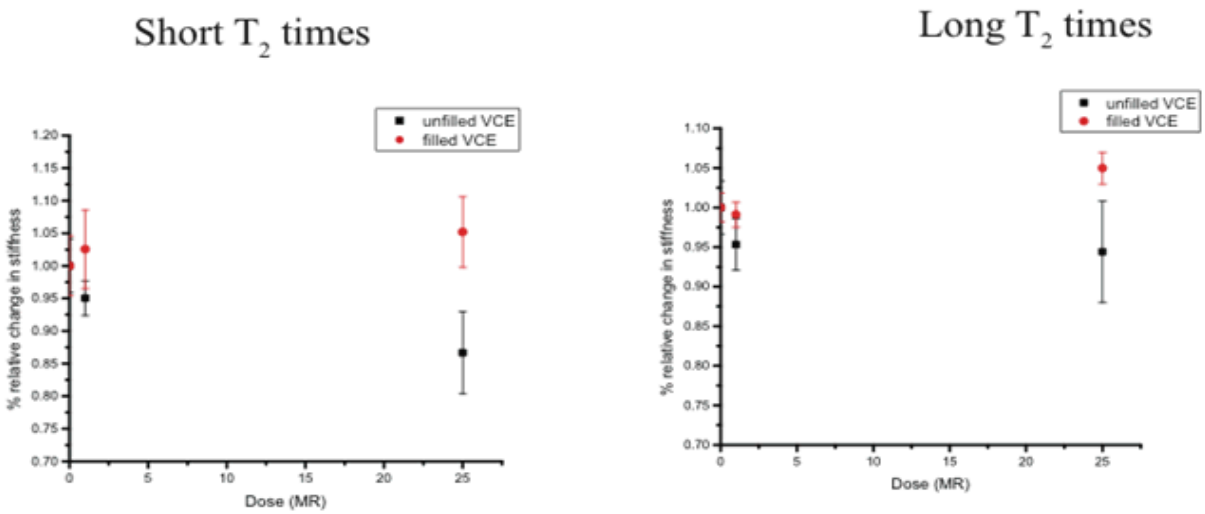

Figure 10: Relative changes in stiffness of irradiated filled and unfilled VCE.

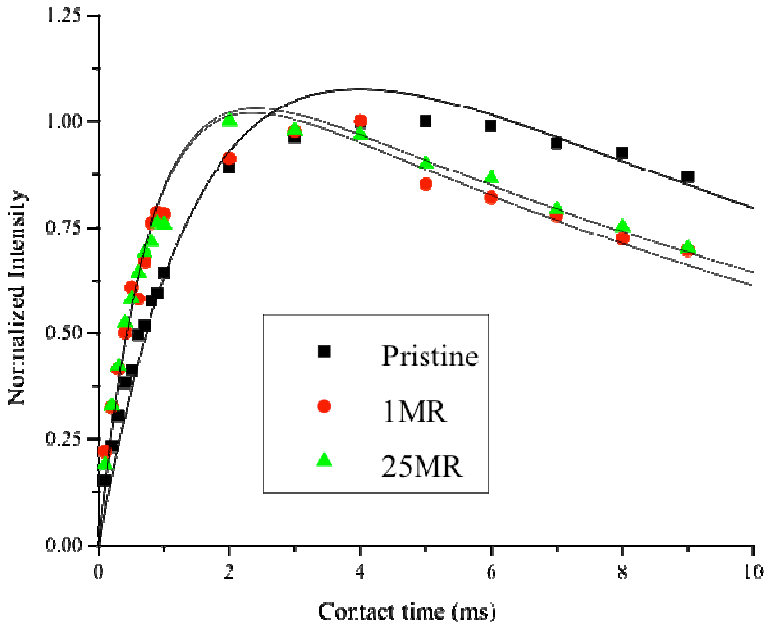

Figure 11: $^{13}C\{^{1}H\}$ CPMAS NMR contact time array on unfilled pristine, 1 MRad and 25 MRad-irradiated VCE.

Table 3. τ_{CH} and τ_{1r} obtained from a $^{13}C\{^1H\}$ CPMAS NMR contact time array.

Sample	τ_{CH} (ms)	$\tau_{1\rho}$ (ms)
Pristine unfilled VCE	1.7	29
1 MR unfilled VCE	0.8	29
25 MR unfilled VCE	0.8	29

To further understand the dynamics of the hard polymers, Center Band-Only Detection of Exchange (CODEX), which enables the characterization of slow segmental reorientation [20-21], was performed on unfilled pristine and 25 MRad-irradiated VCE samples (a simple pulse program is shown in Figure 12). In a CODEX experiment, after the cross-polarization of ^1H to ^{13}C, the NMR magnetization evolves under anisotropic chemical shifts and is re-coupled by a series of 180 degree pulses, which are spaced by a rotor period time ($\tau_r/2$). Then, the magnetization is stored by a time τ_m. Here, motion of the magnetization occurs. A series of phase shifts filter out the slow segmental motion during the 2nd re-coupling pulse (another series of 180 degree pulses, which are spaced by a rotor period time ($\tau_r/2$)). Then, the magnetization is stored along the z-axis during τ_z. We initially tried the CODEX experiments in a 4 mm probe, however the difference in the slow segmental motion was too small to observe a signal. With the new 7 mm DOTY probe, it now takes on the order of two hours to see a small signal with a τ_m=30 μs and τ_z=200 ms and to run a full set of CODEX NMR experiments on these materials would take weeks. We therefore only performed simple CODEX NMR experiments on pristine and 25 MRad-irradiated VCE (Figure 13), which showed no significant differences.

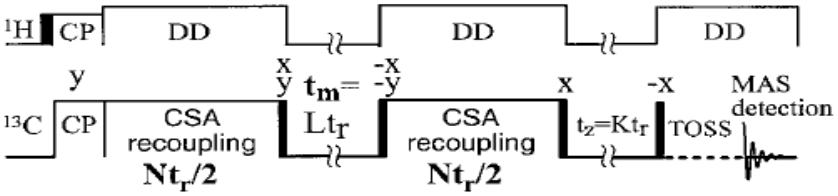

Figure 12: Simplified CODEX pulse program.

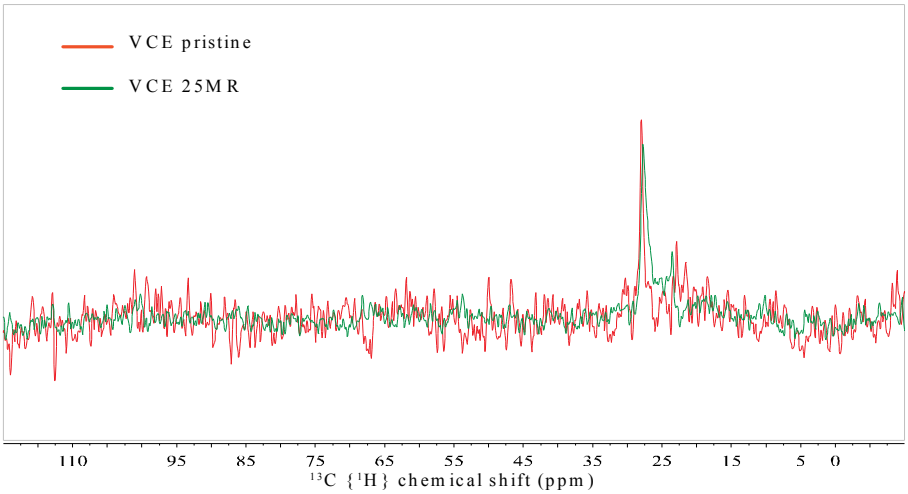

Figure 13: $^{13}C\{^1H\}$ CODEX NMR experiment on pristine and 25 MRad-irradiated VCE.

$^{13}C\{^{1}H\}$ Wide-line-Separation (2D-WISE) and Center band-Only Detection of Exchange (CODEX), showed no significant change between pristine and gamma-irradiated VCE up to 25 MRad, which confirmed the overall structural robustness observed with other methods. Cross-polarization experiments showed a slight decrease in T_{CH} with irradiation, which may be attributed to a decrease in motion (hardening) in the irradiated samples.

3.1.1.4. Mechanical Testing

Mechanical testing was performed on both filled and unfilled VCE samples irradiated with 0, 1 and 25 MRad doses. Mechanical measurements were made on an Instron (Model 5500-R) using a 10 lb load cell equipped with pneumatic grips. Test samples were cut from the pristine or irradiated material to ASTM D-638 Type V dogbones using a punch. Materials were assumed to have a nominal thickness of 30 mils (0.762 mm). Testing was run using a grip separation of 25.4 mm, which was used as the gage length for all calculations. For each sample (material/preparation condition), 5 specimens (replicates) were tested to failure at a crosshead speed of 0.5 in/minute.

No statistical difference between pristine and irradiated samples was observed for unfilled VCE samples, but filled VCE samples showed a decrease in elongation to break and an increase in Young's modulus upon gamma irradiation. These results are consistent with NMR cross-polarization experiments, which indicated an increased hardening of the VCE material with gamma irradiation.

Table 4. Summary of mechanical testing results for filled and unfilled VCE samples exposed to 0, 1 and 25 MRad gamma radiation doses. Each value is the average of measurements performed on 5 replicate samples. Corresponding standard deviations are provided for each value.

Sample	Extension at break (mm)		Force at break (lbs)		Strain at break (in/in)		Tensile strength (psi)		Yong's modulus (psi)	
	Av.	STD	Av.	STD	Av.	STD	Av.	STD	Av.	STD
Unfilled 0 MR	2.81	0.92	2.62	0.78	2.81	0.92	697	207	680	27
Unfilled 1 MR	3.14	0.24	3.33	0.28	3.14	0.24	887	74	661	26
Unfilled 25 MR	2.54	0.33	3.08	0.52	2.54	0.33	822	137	690	17
Filled 0 MR	0.27	0.01	4.44	0.02	0.27	0.01	1183	4	10971	679
Filled 1 MR	0.26	0.01	4.17	0.08	0.26	0.01	1112	22	10872	890
Filled 25 MR	0.20	0.01	4.05	0.05	0.20	0.01	1078	14	12205	578

3.1.2. Chemical effects

3.1.2.1. Infra-Red Spectroscopy (IR)

A Perkin Elmer GX IR spectrometer fitted with an ATR (Attenuated Total Reflectance) accessory with a pressure applicator set to 1 Kg was used to record spectra of unfilled VCE samples. Spectra are presented in Figure 14 and indexed according to modes detailed in Table 5. While no noticeable changes were observed between 0 and 1 MRad, changes were observed after exposure of the samples to a 25 MRad dose. As highlighted in Table 5, changes were observed in the methylene backbone deformation modes, C-O stretch modes of the alcohol groups, and aromatic and N-H bending modes (minor change). Since no change was observed in the O-H stretch modes of the vinyl alcohol group, the change in the C-O stretch modes observed in this group is believed to be a result of the methylene backbone deformation, which is itself associated with the hardening of the material measured by NMR cross-polarization experiments and confirmed by mechanical testing.

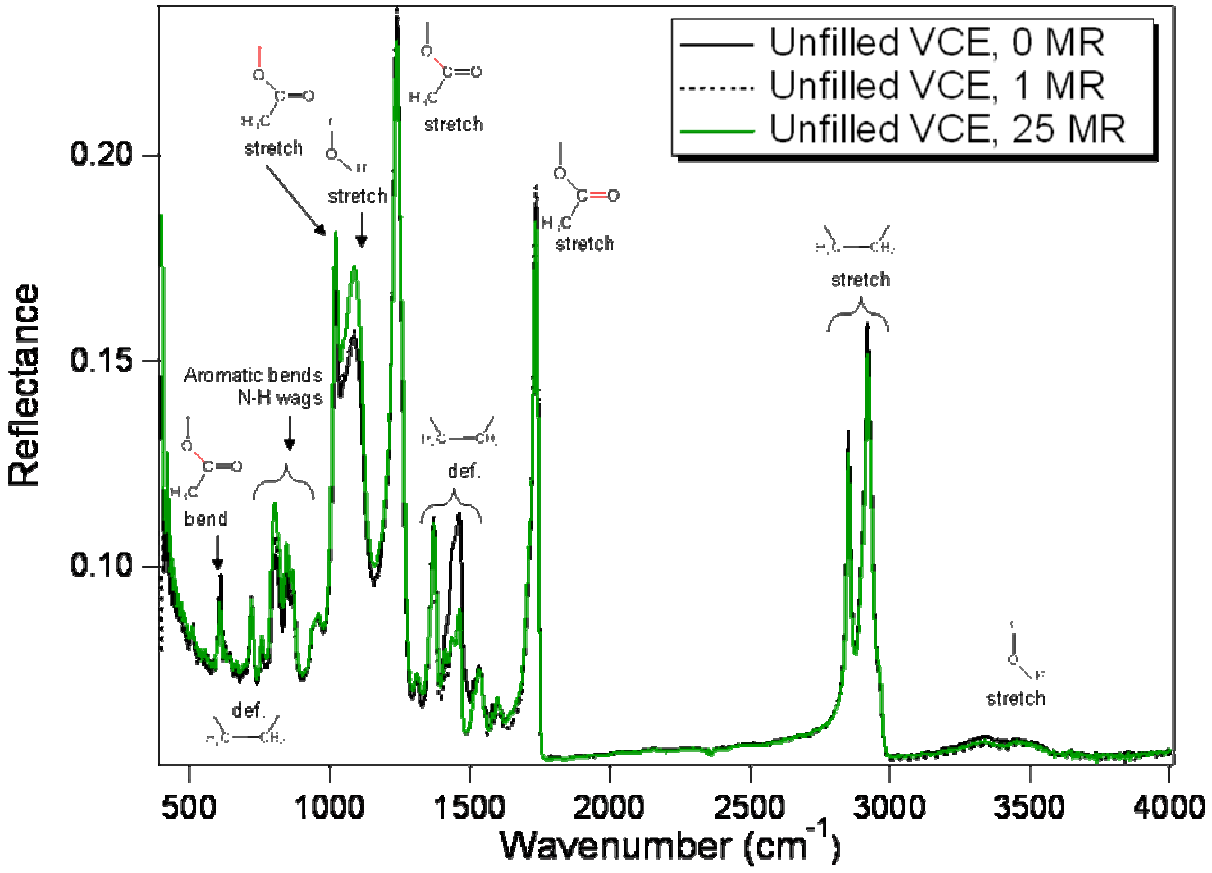

Figure 14: IR reflectance spectra of unfilled VCE samples after exposure to 0, 1 and 25 MRad doses of gamma radiation. Peaks are indexed according to Table 5.

Table 5. List of major IR peaks recorded in spectra from Figure 14, and their respective indexation. Peaks showing changes in intensity upon gamma irradiation are highlighted.

Peak position (cm^{-1})	Indexation
3500-3200	O-H stretches (alcohol group)
2919, 2850	Methylene stretches (polymer backbone)
1735	Carbonyl stretch (acetate group)
1462, 1371	Methylene deformation (polymer backbone)
1238	C-O stretch (acetate group)
1085	C-O stretch (alcohol group)
1019	C-O stretch (polymer link to acetate group)
845-804	Aromatic bends
719	Methylene deformation (polymer backbone)
608	C-O bend (acetate group)

3.1.2.2. Nuclear Magnetic Resonance (NMR)

The pristine, 1 MRad and 25 MRad-irradiated VCE samples were analyzed with ^{13}C, ^{13}C $\{^{1}H\}$ CP, and ^{1}H MAS NMR, using a Bruker Avance 400 MHz spectrometer with a magnetic field of 9.4 T, which gives a resonance frequency of 100.614 MHz for ^{13}C (spin=1/2) and 400 MHz for ^{1}H (spin=1/2). The solid samples were placed at the center of a 4 mm Bruker rotor and spinning rates of 12 kHz were used. The ^{13}C CPMAS spectra were recorded with a cross polarization experiment [13]. The ^{13}C $\{^{1}H\}$ CPMAS NMR data were recorded with a 90 degree pulse width of 5 μs. In these experiments, the relaxation delay was 3 s, the number of acquisitions was 4096 and the contact time was set to 1 ms. The ^{13}C MAS NMR data were recorded with a 90 degree pulse width of 5 μs. In these experiments, the relaxation delay was 10 s and the number of acquisitions was 2048. The ^{1}H MAS NMR data were recorded with a 90 degree pulse width of 5.35 μs. In these experiments, the relaxation delay was 3 s and the number of acquisitions was 32. The ^{3}C $\{^{1}H\}$ CP and ^{13}C MAS NMR data were referenced to glycine at 32 ppm and 176.5 ppm and the ^{1}H MAS NMR data were referenced to TMS at 0 ppm.

Figure 15 shows ^{13}C $\{^{1}H\}$ CP MAS NMR spectra of unfilled pristine, 1 MRad, and 25 MRad-irradiated VCE samples. The ^{13}C $\{^{1}H\}$ CP MAS spectra of both samples show a peak at 20.3 ppm, which represents aliphatic carbon in the form of CH_3. In addition, the spectra show peaks at 25 ppm, 30 ppm, 32 ppm, and 34 ppm, which represent aliphatic carbons in the form of CH_2. ^{13}C $\{^{1}H\}$ CP MAS NMR spectra for the pristine, 1 MRad, and 25 MRad-irradiated VCE samples showed no significant changes in chemical shift or peak shape, indicating that the aliphatic carbons are very stable and are not significantly impacted by exposure to radiation. However, there are small but consistent changes in the CH_2 groups, labeled 4 and 5 in Figure 15, which might indicate that there exists small changes in the mobility of the C-O bonds attached to the aliphatic carbons. The IR data, which is described in the previous section, also observed similar changes in the methylene backbone deformation modes, and C-O stretch modes of the alcohol groups. Finally, the spectra show peaks at 71 ppm and 74 ppm, which represent aliphatic carbon in the form of CH. These were not significantly affected by gamma radiation.

To understand how the carbonyl and aliphatic carbons are affected by irradiation, a ^{13}C MAS NMR experiment was performed on the pristine, 1 MRad, and 25 MRad-irradiated VCE samples. These spectra, presented in Figure 16, show an additional peak at 169 ppm, which represents the carbonyl carbon (Note: there is a background peak due to the NMR probe at

approximately 128 ppm). This peak showed no change in chemical shift or peak shape upon gamma irradiation, which indicates that the carbonyl carbons are very stable and are not significantly impacted by radiation.

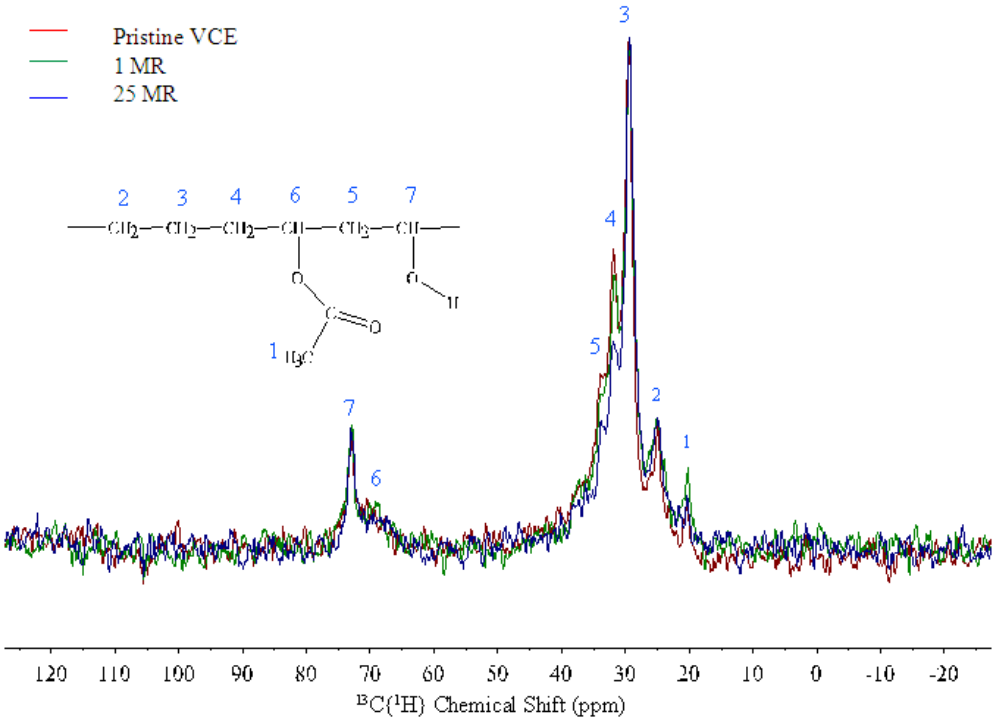

Figure 15: $^{13}C\{^{1}H\}$ CPMAS NMR of unfilled pristine, 1 MRad, and 25 MRad-irradiated VCE samples.

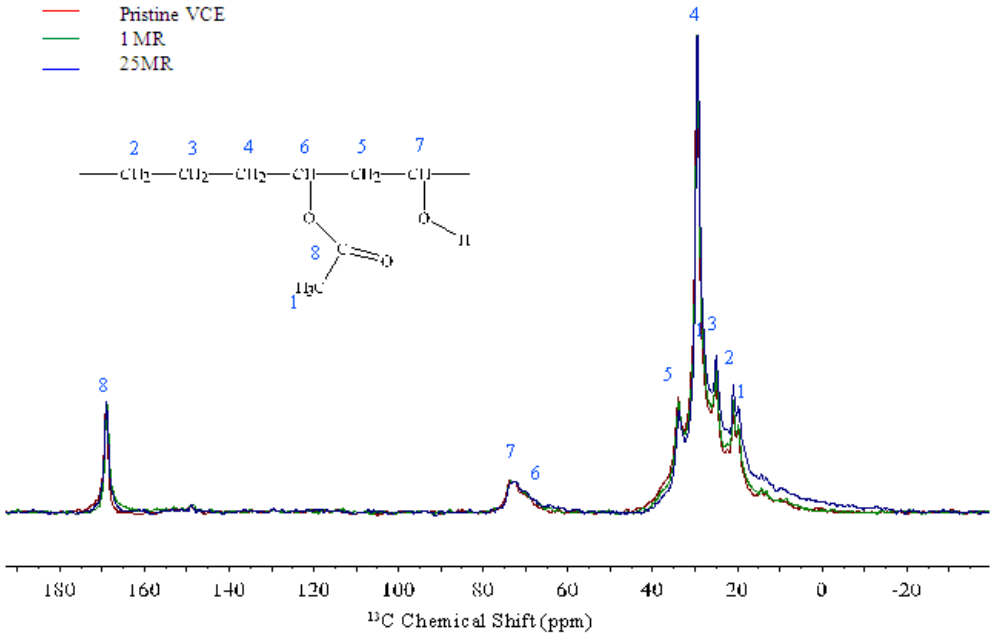

Figure 16: ^{13}C MAS NMR of unfilled pristine, 1 MRad, and 25 MRad-irradiated VCE samples.

However, the aliphatic carbons are more mobile and represent a weak chain when exposed to high levels of radiation and temperature. To verify the changes in the aliphatic carbon in the form of CH, a ^{1}H MAS NMR experiment was performed on pristine, 1 MRad and 25 MRad-irradiated VCE samples (Figure 17). The ^{1}H MAS spectra show a peak at 1.98 ppm, which represents aliphatic protons in the form of CH_3. In addition, spectra show a large peak at 1.33 ppm, which represents aliphatic protons in the form of CH_2. These spectra showed no significant changes in chemical shift or peak shape, indicating that the aliphatic protons are very stable. Similar experiments were performed with filled VCE material with similar results (Figure 18).

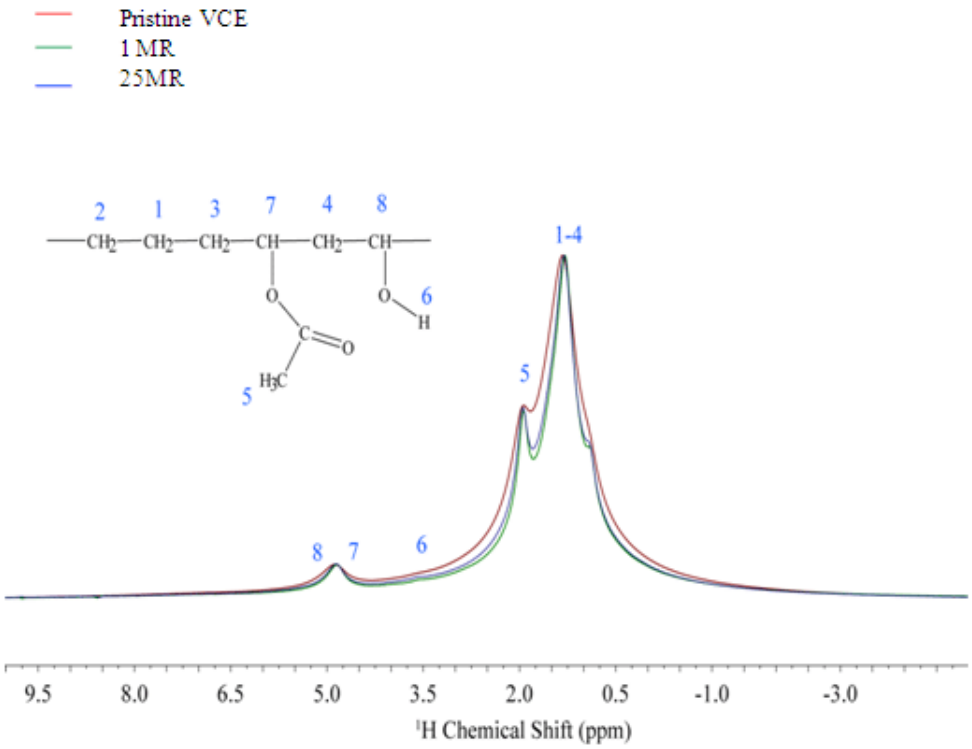

Figure 17: ^{1}H MAS NMR of unfilled pristine, 1 MRad, and 25 MRad-irradiated VCE samples.

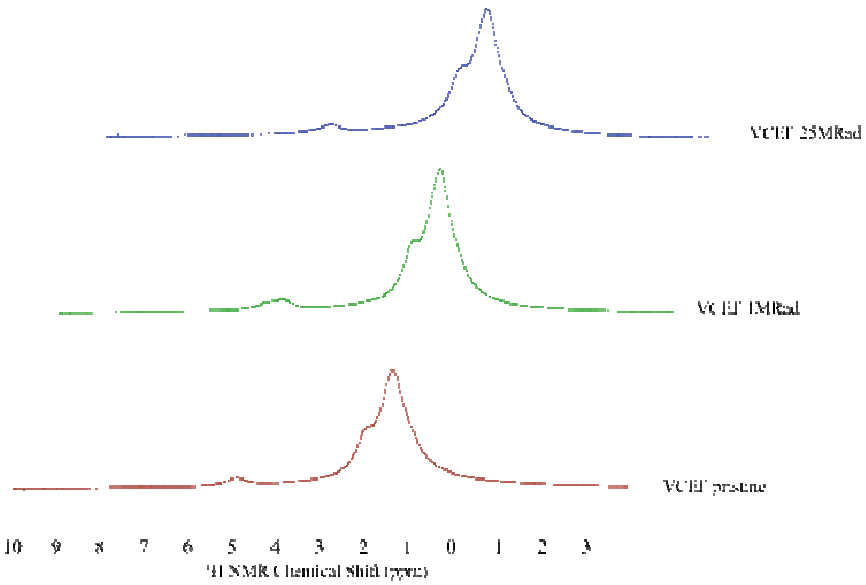

Figure 18: ^{1}H MAS NMR of filled pristine, 1 MRad, and 25 MRad VCE samples.

The various NMR techniques used for this study, including ^{13}C, ^{13}C {^{1}H} CP, and ^{1}H MAS NMR showed no significant changes between pristine and gamma-irradiated VCE up to 25 MRad, which confirmed the chemical robustness observed with other methods.

3.1.2.3. Solid Phase Microextraction – Gas Chromatography/Mass Spectrometry (SPME-GC/MS)

Filled and unfilled VCE samples (20-30 mg each) were placed in SPME headspace vials (20mL), and sealed with crimp caps and septa (20 mm, Teflon/blue silicone, level 4) that were purchased from MicroLiter Analytical Supplies. For each sample type, 5 replicates were left at room temperature and another 5 replicates were placed in an oven at 150 ºC. All samples remained at their designated temperatures for two weeks. An additional set of blanks (sealed empty vials) was also prepared for storage at room temperature and 150 ºC prior to SPME sampling. The storage at elevated temperatures was performed to maximize the volatilization of degradation signatures for observation by SPME sampling, while retaining a room temperature sample and a blank to serve as controls.

The samples were analyzed by SPME GC/MS using an automated system under the following conditions: 85 m Carboxen/PDMS SPME fiber (purchased from Supelco), conditioned between samples for 5 min at 260 ºC; headspace sampled at 50 ºC for 20 min and injected into the GC for 1 min at 250 ºC. The Agilent 6890 GC was set for splitless injection and purged at 0.5 min using a J & W Scientific DB-624 column (30 m, 0.25 mm ID, 1.4 m film) with a constant 1.0 mL/min flow of helium. The 20 min run had the following temperature profile: 40 ºC /1.05 min, 23.41 ºC /min to 260 ºC, and held 6.81 min. An Agilent 5973 mass spectrometer scanned the mass range from 35-450 at a rate of 1.81 scans/s with no filament delay. Outgassing products were identified by comparison of their mass spectra to the NIST 02 mass spectral library.

Figure 19 shows GC-MS spectra of unfilled VCE. The nature and abundance of the chemicals found in the headspace for both filled and unfilled materials is summarized in Table 6.

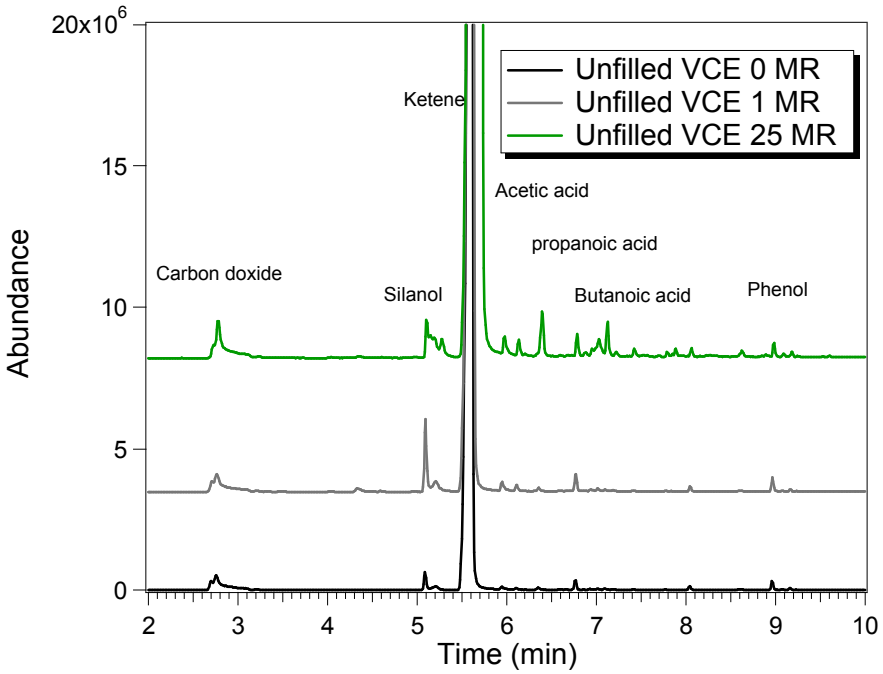

Figure 19: SPME-GC-MS spectra of pristine and gamma-irradiated VCE samples at 150˚C.

Table 6. Summary of SPME-GC-MS experiments, comparing abundance (%) of outgassing products from both pristine and irradiated VCE at room temperature and 150 ˚C.

Unfilled VCE	**0 MRad**		**1 MRad**		**25 MRad**	
Chemical	**RT**	**150 ºC**	**RT**	**150 ºC**	**RT**	**150 ºC**
Ketene	0	6.28	0	9.3	0	16.3
Acetic acid	1.2	0	7.4	0.1	24.5	14.2
butanoic acid	0	0	0	0	0.4	0.4
Propanoic acid	0	0	0	0	0.2	0.5
Silanol	1.1	1.6	0.6	2.8	0	0.8
Phenol	0	0.3	0	0.35	0.2	0.15
Carbon dioxide	0	0.4	0	0.7	0	0.7

Filled VCE	0 MRad		1 MRad		25 MRad	
Chemical	**RT**	**150 ºC**	**RT**	**150 ºC**	**RT**	**150 ºC**
Ketene	0	18.6	0	15.5	0	7.93
Acetic acid	1.2	22.3	5.7	14.2	43.2	13.4
Butanoic acid	0	0.5	0	0.5	1.3	0.7
Propanoic acid	0	0.6	0	0.7	0.8	0.9
Silanol	0	0.2	0.7	1.7	2	2
Phenol	0	0.15	0.3	0.15	0.8	0.15
Carbon Dioxide	0	0.7	0	0.6	0	1.1

The main outgassing chemicals are: ketene, acetic acid, butanoic acid, propanoic acid, silanol, phenol and carbon dioxide. Acetic acid, which is released in large abundance upon temperature and/or gamma irradiation, is the product of the hydrolysis of the vinyl acetate groups of VCE (see VCE structure shown in Figure 20) into vinyl alcohol groups. Propanoic and butanoic acids only appear in low abundance at high temperature and/or high gamma irradiation doses and are probably the combination of the acetic acid with chain fragments. Ketene is only observed at high temperature while acetic acid is outgassed at room temperature, indicating that ketene is most probably a high temperature degradation product of acetic acid (ketene is a well-known product of the pyrolysis of acetic acid). Phenol and carbon dioxide, which are released in low abundance, are degradation products of the crosslinking agent Hylene MP (see structure in Figure 21) used in the synthesis of VCE, resulting from thermal unblocking or from hydrolysis of urethane. Silanol most probably comes from the outgassing of silicone mold release used during the processing of the VCE samples.

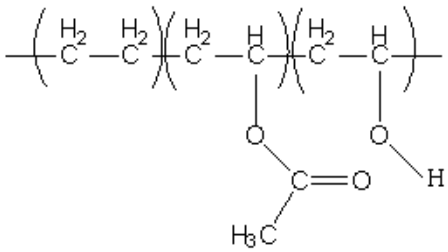

Figure 20: Chemical structure of VCE terpolymer.

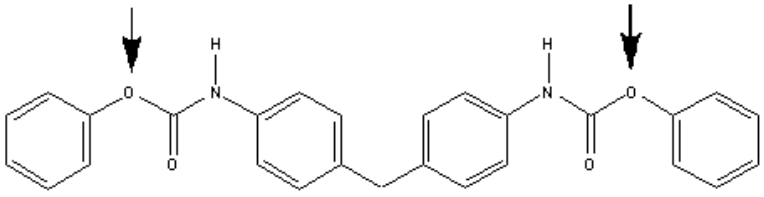

Figure 21: Chemical structure of Hylene MP curing agent (diphenol-4,4', -methylenebis(phenylcarbamate). Arrows indicate the 2 sites where a hydrolysis reaction may lead to the formation of phenol molecules.

As may be seen in the first columns of Table 6, outgassing of unfilled and filled VCE under normal conditions (room temperature, no gamma irradiation) is negligible (only very low levels of acetic acid and silanol are observed). Gamma irradiation and thermal treatment to 150 ºC mainly increase the release of acetic acid and ketene.

3.1.2.4. Phenol extraction followed by HPLC

VCE samples were sonicated in acetonitrile for 3 hrs and then let to rest in acetonitrile for 13 hrs prior to HPLC analysis following protocol LTM 3905-B provided by the Kansas City Plant [22]. Table 7 summarizes the results obtained on both filled and unfilled samples. HPLC analysis confirmed that the quantity of phenol released is low (tens of ppm after vigorous extraction), and that it slightly increases upon gamma irradiation, as observed via SPME-GC-MS. This observation confirmed the effectiveness of the 'phenol bake-out' process performed by the Kansas City Plant to remove phenol produced during the VCE curing reaction (see Figure 2).

Table 7. Summary of phenol extraction and HPLC measurements on filled and unfilled VCE.

Sample	Sample Wt. (g)	Volume Acetonitrile (µL)	Analysis Conc. (µg/mL)	Phenol (ppm)	Phenol Average (ppm)	Std. Dev.
VCE (Unfilled) 0 MR	0.1320	1320	2.373	23.73		
VCE (Unfilled) 0 MR	0.1328	1328	2.274	22.74		
VCE (Unfilled) 0 MR	0.1323	1323	2.042	20.42	**22.3**	1.7
VCE (Unfilled) 1 MR	0.1306	1306	1.870	18.70		
VCE (Unfilled) 1 MR	0.1303	1303	2.068	20.68		
VCE (Unfilled) 1 MR	0.1275	1275	2.047	20.47	**20.0**	1.1
VCE (Unfilled) 25 MR	0.1306	1306	4.941	49.41		
VCE (Unfilled) 25 MR	0.1252	1252	4.496	44.96	**47.2**	3.1
VCE (Filled) 0 MR	0.1651	1651	0.484	4.84		
VCE (Filled) 0 MR	0.1661	1661	0.483	4.83		
VCE (Filled) 0 MR	0.1740	1740	0.481	4.81	**4.8**	0.01
VCE (Filled) 1 MR	0.1933	1933	0.787	7.87		
VCE (Filled) 1 MR	0.1951	1951	0.802	8.02		
VCE (Filled) 1 MR	0.2020	2020	0.583	5.83	**7.2**	1.22
VCE (Filled) 25 MR	0.1881	1881	3.936	39.36		
VCE (Filled) 25 MR	0.1851	1851	3.585	35.85		
VCE (Filled) 25 MR	0.1852	1852	3.433	34.33	**36.5**	2.6

3.2. Thermal degradation of VCE

Unfilled VCE samples were thermally aged in air using a muffle furnace at 50, 100, 125, 150, 175, 200, 250 and 300 ºC. Upon thermal treatment, the sample's appearance changed from clear to dark yellow (175 ºC) and then to black (250 ºC), as may be seen on Figure 21. No noticeable changes in size, color, texture and flexibility were observed for thermal treatments up to 150 ºC. At 175 ºC, the sample started to change color and warp, and at 250 ºC, the sample became black and its surface started to show cracks. At 300 ºC, the sample broke into pieces and lost mass, which correlates with TGA results shown on Figure 23, indicating a 30 % mass loss after the scission of the acetate groups around 300-320 ºC.

UV-vis absorption spectroscopy was performed on unfilled samples in order to spectrally characterize the absorption change (Figure 22). These experiments revealed a broad spectral feature centered at 375 nm after thermal treatment at 200 ºC. Studies of EVA materials used for solar cell encapsulation have shown that EVA turns from clear to yellow-brown after 5 years of weathering [23]. Detailed analysis using a combination of TGA and UV-vis absorption techniques concluded that the yellowing of thermally degraded EVA may be attributed to the formation of polyconjugated bonds $(C=C)_n$, also called polyenes. With increasing temperature, polyenes become longer and the absorption is therefore shifted toward shorter wavelengths (the material changes from light yellow to darker yellow). The formation of polyenes is also attributed to the deacetylation process, which generates acetic acid (as observed via SPME-GS-MS). Other less likely sources of discoloration in VCE are large decomposition products of the Hylene MP cross-linking agent. While mono-substituted benzene rings such as phenol display absorption bands typically below 280 nm, di-substituted benzene rings typically display absorption bands between 280 and 380 nm.

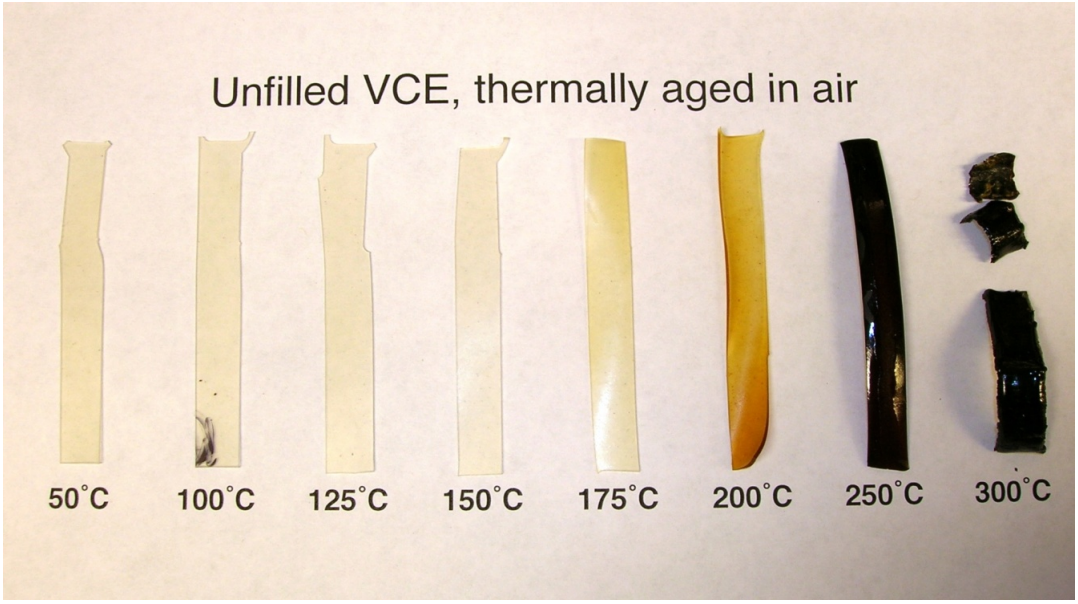

Figure 21: Photograph of unfilled VCE samples after thermal aging in air at 50, 100, 125, 150, 175, 200, 250 and 300 ºC respectively.

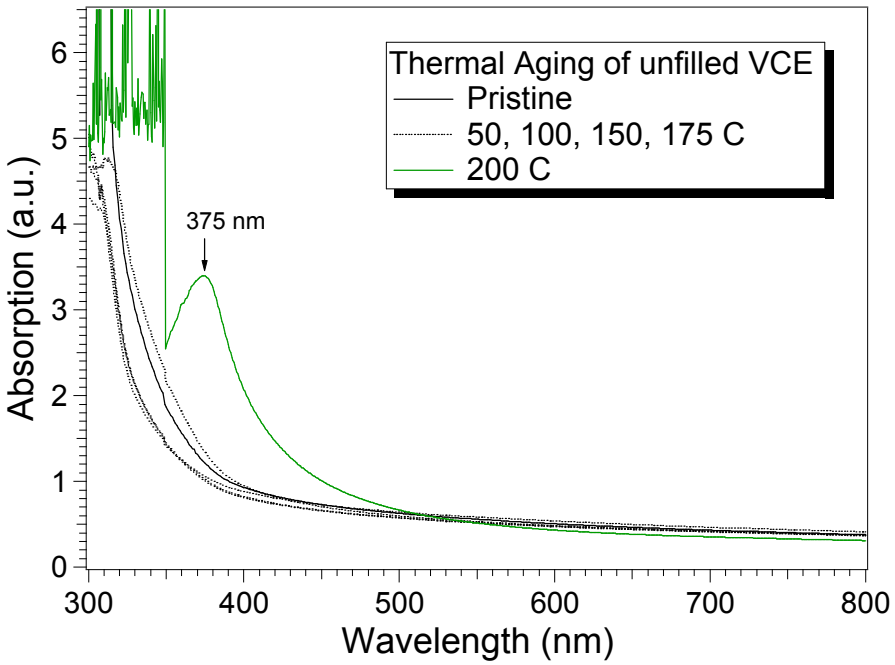

Figure 22: UV-vis absorption spectra of unfilled VCE samples after thermal aging in air at 50, 100, 150, 175, 200 ºC respectively.

3.2.1. Thermogravimetric Analysis (TGA)

TGA experiments were performed on a Perkin Elmer TGA-7, under a flow of argon gas of 20 mL/min. Approximately 3 mg of each sample were heated from 50 ºC to 900 ºC with a ramp rate of 10 ºC /min and the change in weight percent was plotted as a function of temperature (see Figure 23).

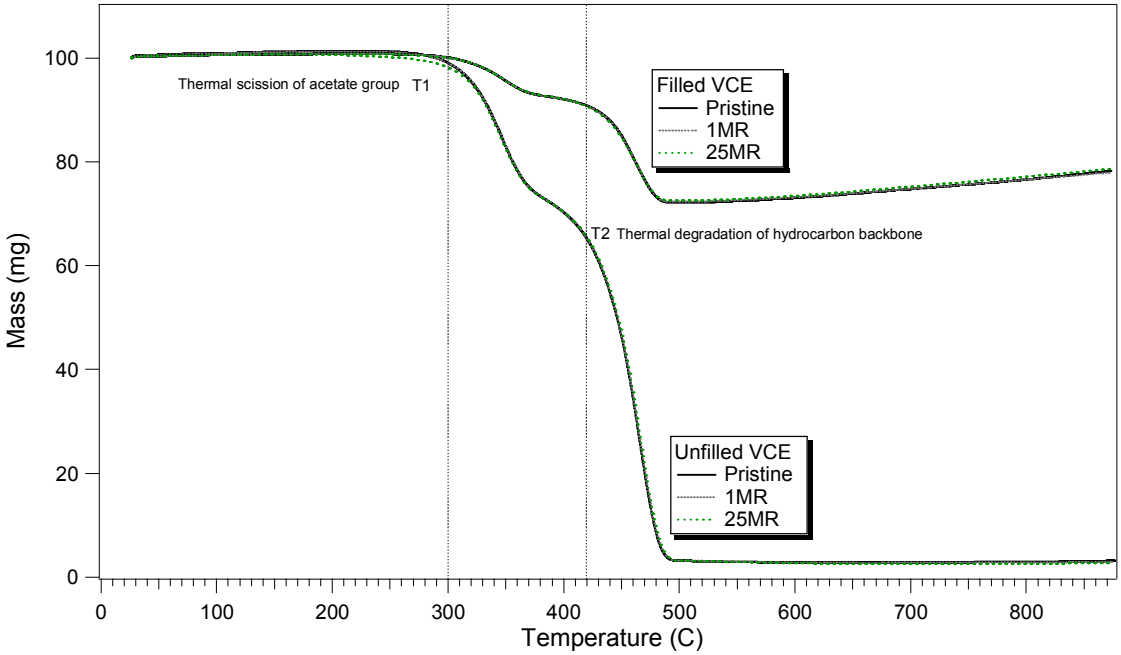

Figure 23: TGA curves for filled and unfilled VCE samples exposed to 0, 1 and 25 MRad gamma radiation doses.

TGA experiments performed on both filled and unfilled VCE samples (Figure 23) showed that no significant thermal degradation occurs below 300 ºC. Thermal scission of the acetate group was observed at 300-320 ºC (see picture of a sample stored in air at 300 C for 12 hrs on Figure 21), followed by the thermal degradation of the hydrocarbon backbone at 420 ºC (main chain degradation). There were no significant differences between the thermal degradation curves of pristine and irradiated VCE. Filled samples retained approximately 70 % of their weight after thermal treatment, which is consistent with the weight fraction of filler particles, which is 70%.

3.2.2. Structural effects

3.2.2.1. Differential Scanning Calorimetry (DSC)

DSC experiments were performed using a Perkin Elmer Pyris Diamond instrument, under a flow of nitrogen gas of 20 mL/min. Sample discs were cut using a 2.5 mm diameter biopsy punch and individual discs were placed into aluminum pans, weighed, and submitted to the following temperature cycle: 2 min at 25 ºC, 25 to 200 ºC at 10 ºC/min, 2 min at 200 ºC, 200 to -60 ºC at 10 ºC/min, 10 min at -60 ºC, and -60 to 200 ºC at 10 ºC/min. Thermograms were base line-corrected to remove the contribution from the aluminum pans.

Heat flow versus temperature curves for the unfilled VCE material subjected to thermal aging in air up to 200 ºC are shown in Figure 24, where each curve represents the average of two replicate samples. Thermograms show multiple and complex melting behaviors for the VCE terpolymer (three peaks), due to overlapping transitions of the monomers. Peaks 1 and 2 are typically attributed to the melting of vinyl acetate domains, while peak 3 corresponds to the ethylene domains [9]. The presence of the second peak for the vinyl acetate domains has been attributed in the literature to defective bundle-like structures in EVA [10].

Table 8 summarizes the data for unfilled samples in terms of enthalpy of fusion and heat capacity. Although thermogram peaks are complex for the VCE terpolymer, DSC experiments (Figure 24) revealed small but consistent differences between pristine and thermally aged, unfilled VCE samples including: an increase of the melting transition temperature (T_m), which indicates a change in mobility, a decrease in enthalpy of fusion (ΔH_f), which indicates a decrease in crystallinity after irradiation, and finally, broadened transitions (larger peak areas), which indicates less uniformity.

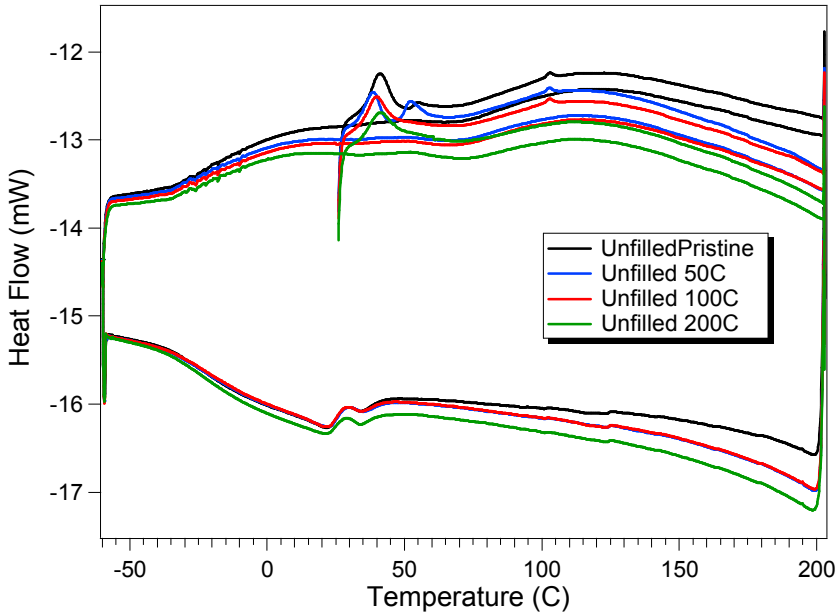

Figure 24: DSC curves for thermally-aged unfilled VCE samples. Each curve represents the average of two replicate samples.

Table 8. Quantitative summary of DSC experiments, comparing properties of pristine and thermally-aged unfilled VCE samples.

Specimen	Weight (mg)	Peak Location (°C)	Peak Area (mJ)	ΔH (J/g)	T_g (°C)	ΔC_p (J/g-°C)
Pristine	3.6	40.9	21.1	**5.9**	-14.8	**0.76**
50°C	3.7	38.4 / 52.2	16.2 / 7.3	4.4/2.0	-11.3	0.72
50°C	3.8	38.5 / 52.2	13.2 / 6.4	3.5/1.7	-12.6	0.77
50°C av.				**3.9/1.8**		**0.74**
100°C	3.6	39.6	16.6	4.6	-10.9	0.68
100°C	3.8	39.6	17.4	4.6	-11.3	0.70
100°C av.				**4.6**		**0.69**
125°C	3.8	39.6	16.6	4.4	-13.0	0.76
125°C	3.7	39.6	18.2	4.9	-12.4	0.73
125°C av.				**4.6**		**0.74**
150°C	3.5	39.8	17.1	4.9	-13.2	0.90
150°C	3.9	40.0	16.8	4.3	-14.6	0.76
150°C av.				**4.6**		**0.83**
175°C	3.6	40.1	14.5	4.0	-13.1	0.79
175°C	3.5	40.1	14.1	4.0	-13.0	0.76
175°C av.				**4.0**		**0.77**
200°C	3.7	41.2	16.4	4.4	-13.2	0.79
200°C	3.8	41.0	17.1	4.5	-13.4	0.72
200°C av.				**4.4**		**0.75**

3.2.2.2. Nuclear Magnetic Resonance (NMR)

To explore changes in mobility and stiffness of the VCE material upon temperature aging, we performed spin-spin relaxation (T_2-relaxation) NMR experiments on unfilled VCE exposed to various temperatures, including 50°C, 125°C, 150°C, 175°C, 200°C, 250°C and 300°C. T_2 relaxation is inversely correlated to the relative stiffness of the bulk material. The data shows a double exponential, with a short and a long component (Figure 25). The short component of the T_2 relaxation shows a slight decrease in stiffness with increased temperature while the long component shows a slight increase in stiffness with increased temperature. Overall, T_2 experiments showed no significant change in mobility or stiffness of VCE upon thermal aging.

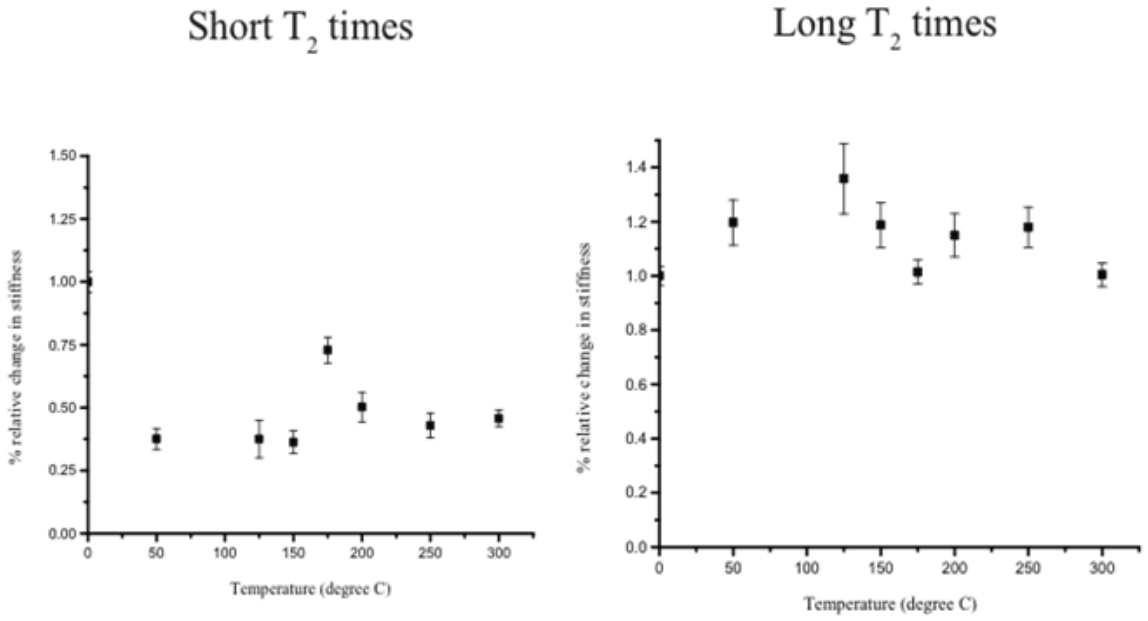

Figure 25: Relative changes in stiffness of unfilled VCE exposed to various temperatures.

3.2.3. Chemical effects

3.2.3.1. Infra-Red Spectroscopy (IR)

A Perkin Elmer GX IR spectrometer fitted with an ATR (Attenuated Total Reflectance) accessory with a pressure applicator set to 1 Kg was used to record spectra on unfilled VCE samples. Spectra are presented in Figure 26 and indexed according to modes detailed in Table 9. As highlighted in Table 9, changes were observed in the methylene backbone deformation modes, C-O and O-H stretch modes of the alcohol groups, and aromatic and N-H bending modes (minor change). Since changes observed in the O-H and C-O stretch modes of the vinyl alcohol group are not correlated to temperature, and since there is no significant loss of the O-H stretch

mode, it is believed that they might be a result of the small methylene backbone deformation. NMR also showed small changes in the mobility of the C-O bonds attached to the aliphatic carbons upon thermal aging.

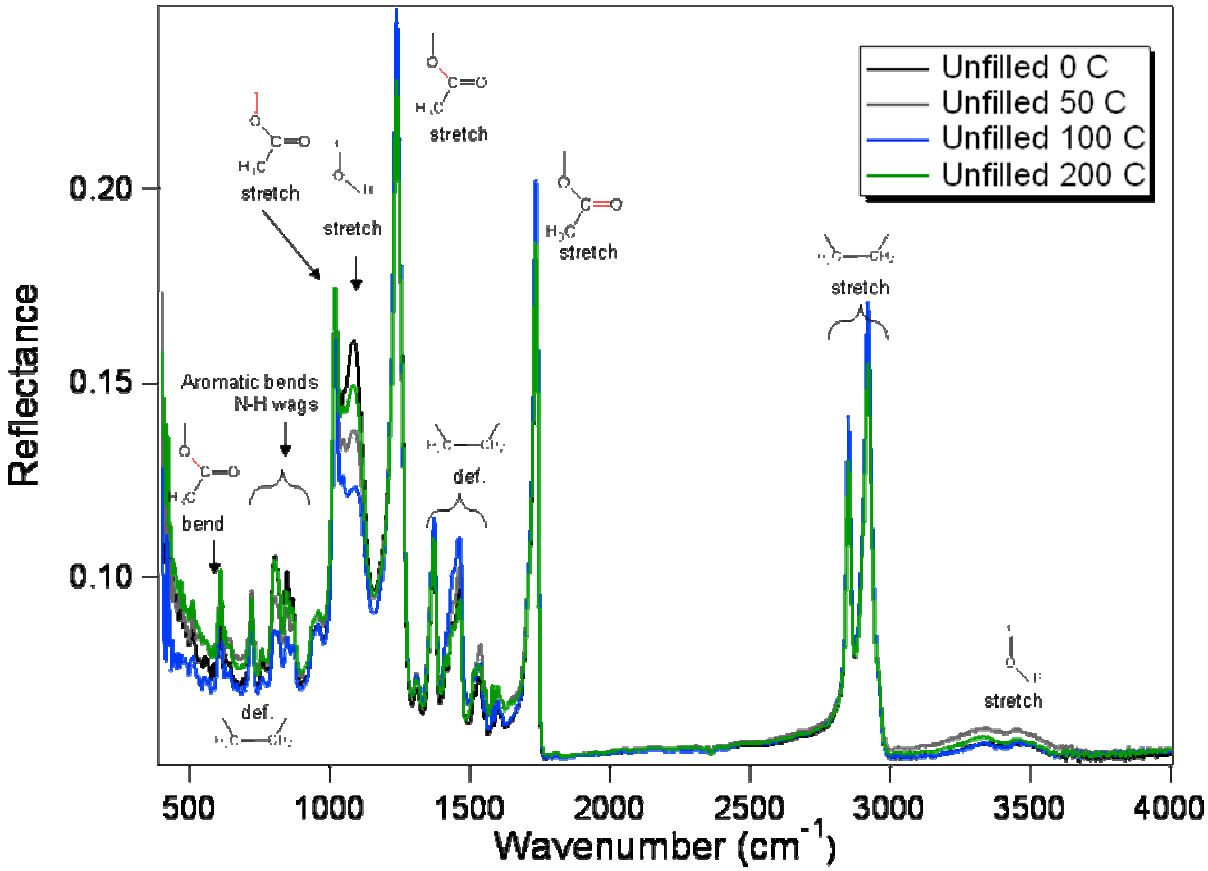

Figure 26: IR reflectance spectra of unfilled VCE samples after thermal aging in air at 50, 100 and 200 ºC respectively. Peaks are indexed according to Table 9.

Table 9. List of major IR peaks recorded in spectra from Figure 26, and their respective indexation. Peaks showing changes in intensity upon thermal aging are highlighted.

Peak position (cm^{-1})	Indexation
3500-3200	O-H stretches (alcohol group)
2919, 2850	Methylene stretches (polymer backbone)
1735	Carbonyl stretch (acetate group)
1462, 1371	Methylene deformation (polymer backbone)
1238	C-O stretch (acetate group)
1085	C-O stretch (alcohol group)
1019	C-O stretch (polymer link to acetate group)
845-804	Aromatic bends
719	Methylene deformation (polymer backbone)
608	C-O bend (acetate group)

3.2.3.2. Nuclear Magnetic Resonance (NMR)

^{1}H MAS NMR was used to investigate thermal degradation of unfilled VCE at 50°C, 125°C, 150°C, 175°C, 200°C, 250°C and 300°C (Figure 27). The ^{1}H MAS spectra showed a peak at 1.98 ppm, which represents aliphatic protons in the form of CH_3. In addition, the spectra showed a large peak at 1.33 ppm, which represents aliphatic protons in the form of CH_2. No significant changes in chemical shift or peak shape were observed upon thermal aging, indicating that the aliphatic protons are very stable. However, slight changes between 5-6 ppm were observed on VCE samples exposed to temperatures above 175°C, which correspond to protons in the alcohol and acetate groups (IR data also showed small changes in the alcohol groups). The large peak between 4 and 5 ppm observed on the sample heated to 175°C, appears to be an anomaly.

^{13}C {^{1}H} CP MAS NMR and ^{13}C MAS NMR performed on pristine and thermally aged VCE (50°C and 250°C) showed no significant changes (Figure 28 and 29), confirming the chemical stability of VCE against thermal treatments. Only slight changes were observed in the ^{13}C {^{1}H} CP MAS NMR for the CH_2 groups, labeled 4 and 5 (Figure 28), which might indicate that there exists small changes in the mobility of the C-O bonds attached to the aliphatic carbons. The IR data, which is described in the previous section, showed similar changes in the methylene backbone deformation modes, and C-O stretch modes of the alcohol groups.

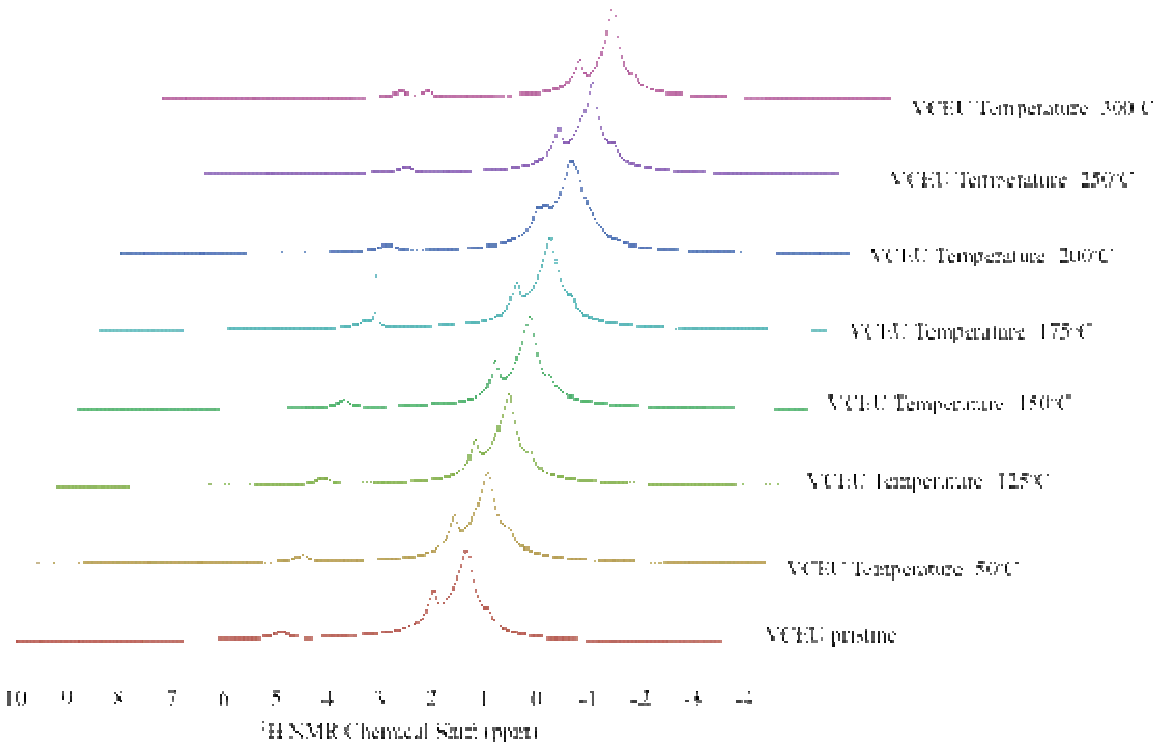

Figure 27: ^{1}H MAS NMR of unfilled VCE exposed to 50°C, 125°C, 150°C, 175°C, 200°C, 250°C and 300°C.

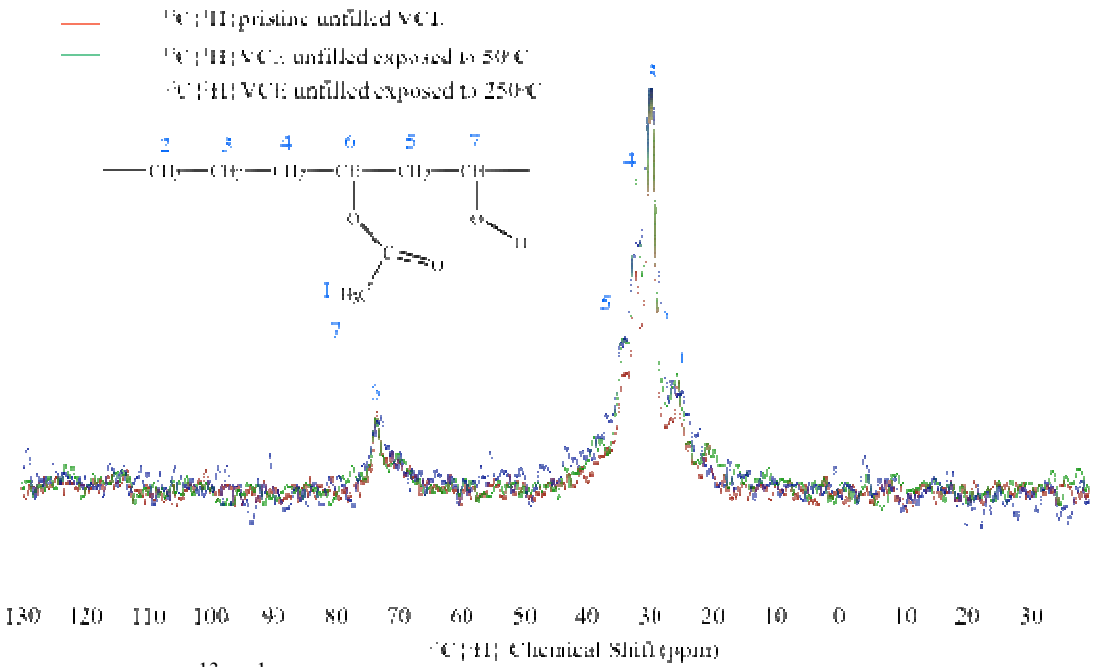

Figure 28: $^{13}C\{^{1}H\}$ CPMAS NMR of unfilled VCE aged at 50°C and 250°C.

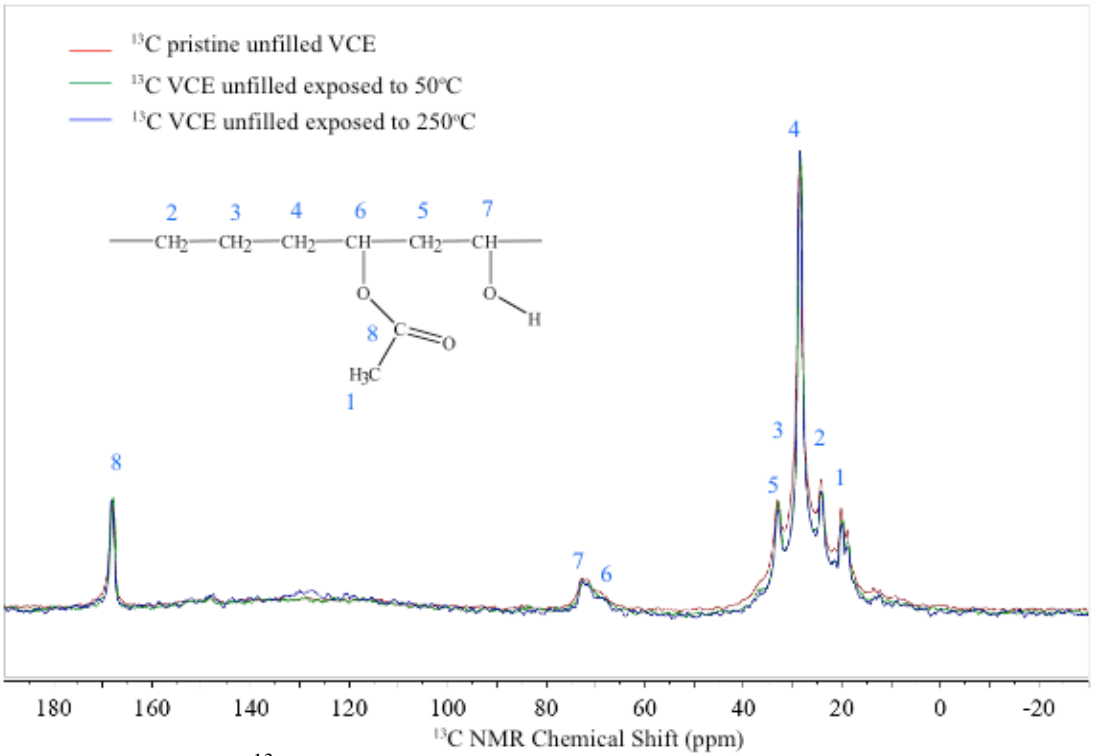

Figure 29: ^{13}C MAS NMR of unfilled VCE aged at 50°C and 250°C.

3.2.3.3. Solid Phase Microextraction – Gas Chromatography/Mass Spectrometry (SPME-GC/MS)

Unfilled VCE samples (20-30 mg each) were placed in SPME headspace vials (20mL), and sealed with crimp caps and septa (20 mm, Teflon/blue silicone, level 4) that were purchased from MicroLiter Analytical Supplies. Since the samples had been thermally aged, only 5 replicates left in SPME vials at room temperature for two weeks were analyzed. An additional set of blanks (sealed empty vials) was also prepared for storage at room temperature prior to SPME sampling.

The samples were analyzed by SPME GC/MS using an automated system under the following conditions: 85 m Carboxen/PDMS SPME fiber (purchased from Supelco), conditioned between samples for 5 min at 260 ºC; headspace sampled at 50 ºC for 20 min and injected into the GC for 1 min at 250 ºC. The Agilent 6890 GC was set for splitless injection and purged at 0.5 min using a J & W Scientific DB-624 column (30 m, 0.25 mm ID, 1.4 m film) with a constant 1.0 mL/min flow of helium. The 20 min run had the following temperature profile: 40 ºC /1.05 min, 23.41 ºC /min to 260 ºC, and held 6.81 min. An Agilent 5973 mass spectrometer scanned the mass range from 35-450 at a rate of 1.81 scans/s with no filament delay. Outgassing products were identified by comparison of their mass spectra to the NIST 02 mass spectral library.

Only acetic acid was found in the headspace of thermally-aged, unfilled VCE material, as may be seen on Table 10. The release of this chemical increased with temperature, reaching high abundance for samples aged at 300 ºC. As previously discussed, acetic acid is the product of the hydrolysis of the vinyl acetate groups of VCE (see VCE structure shown in Figure 20) into vinyl alcohol groups.

Table 10. Quantitative summary of SPME-GC-MS experiments, comparing abundance (%) of outgassing products from both pristine and thermally-aged VCE at room temperature.

Chemical	50 ºC	100 ºC	125 ºC	150 ºC	175 ºC	200 ºC	250 ºC	300 ºC
Acetic acid	0.65	0	0	0	1.9	2.1	21.7	44.9

3.2.3.4. Phenol extraction followed by HPLC

VCE samples were sonicated in acetonitrile for 3 hrs and then let to rest in acetonitrile for 13 hrs prior to HPLC analysis following protocol LTM 3905-B provided by the Kansas City Plant [23]. Table 11 summarizes the qualitative results obtained on unfilled samples. HPLC analysis confirmed that the quantity of phenol released is low (below 10 ppm after vigorous extraction), and that it decreases upon thermal aging (due to the fact that the phenol is outgassed during the thermal aging process, as detected via SPME). Residual phenol levels were below the detection limit of HPLC.

Table 11. Summary of phenol extraction and HPLC measurements on thermally-aged, unfilled VCE samples. Each data point is the average of two replicates.

Sample	Sample Wt. (g)	Volume Acetonitrile (µL)	Analysis Conc. (µg/mL)	Average Phenol (ppm)	Standard deviation
VCE (Unfilled) Pristine	0.1323	1323	2.042	**22.3**	1.7
VCE (Unfilled) 50 C	0.0507	507	0.600	**5.9**	0.2
VCE (Unfilled) 100 C	0.0658	658	0.3	**2.9**	0.1
VCE (Unfilled) 125 C	0.0534	534	0.324	**3.5**	0.4
VCE (Unfilled) 150 C	0.0571	571	0.324	**3.5**	0.4
VCE (Unfilled) 175 C	0.0754	754	0	**0**	-
VCE (Unfilled) 200 C	0.0661	661	0	**0**	-
VCE (Unfilled) 250 C	0.0644	644	0	**0**	-
VCE (Unfilled) 300 C	0.0758	758	ND	**0**	

4. Conclusion

Aging studies of both filled and unfilled VCE samples synthesized, milled, molded and cured at the Kansas City plant using WR-qualified processes were performed in air, using radiation doses up to 25 MRad and temperatures up to 300 ºC. Experiments focused on comparing structural and chemical properties of aged samples to those of pristine VCE material.

NMR and mechanical experiments showed an increased hardening of the VCE material upon gamma irradiation. SPME-GC-MS showed that only acetic acid and silanol outgassed from the samples at room temperature with irradiation doses of 1 MRad, and that acetic acid, butanoic acid (low), propanoic acid (low), silanol (low), phenol (low) and carbon dioxide (low) outgassed with irradiation doses of 25 MRad. Phenol analysis by HPLC confirmed low levels of phenol release (tens of ppm) upon gamma irradiation. Combined IR and NMR spectroscopy results confirmed that the VCE material maintains its overall chemical structure and properties under gamma irradiation (only minor methylene backbone, C-OH group and aromatic ring deformations were observed).

Significant temperature degradation was found to occur above 300 ºC, with the thermal scission of the acetate group observed by TGA between 300 and 320 ºC, followed by the thermal degradation of the hydrocarbon backbone at 420 ºC. DSC experiments showed a small but

consistent decrease in uniformity and mobility upon thermal aging. SPME-GC-MS showed almost no outgassing at room temperature on pristine samples, while ketene, acetic acid, silanol (low), carbon dioxide (low) and phenol (low) outgassed when samples were stored at 150 ºC. The only chemical which continued to outgas at room temperature after thermal aging of the samples at 175 ºC was acetic acid, which is a product of the hydrolysis of the vinyl acetate groups of VCE into vinyl alcohol groups. Phenol analysis by HPLC confirmed very low levels of phenol (< 10 ppm) in thermally aged samples and combined IR and NMR spectroscopy results confirmed that the VCE material maintains its overall chemical structure and properties at temperatures up to 200 ºC (only minor methylene backbone, C-OH group and aromatic ring deformations were observed) .

5. Future work

Next year will focus on performing thorough mechanical testing on all samples, which will provide insight into structural changes. Two VCE part returns have also been requested and will be analyzed alongside pristine VCE manufactured at the Kansas City Plant for both structural and chemical changes. These experiments should lead to a complete model of VCE aging in current systems.

6. References

1. W.E. Cady, *Transition temperatures and crystallinity in EVA, VCE, and Rattan C*, LLNL report UCID-15424 (1969).

2. P.M. Wilson, D.A. Spieker, *Enhanced Surveillance of Filled Elastomers*, KCP report KCP-613-6004 (1997).

3. E.A. Eastwood, D.E. Bowen, *VCE replacement development: characterization of EVA materials*, KCP report KCP-613-6929 (2004).

4. E.A. Eastwood, *VCE replacement development: curing studies*, KCP report KCP-613-8161 (2006).

5. A. Lopez-Rubio, J.M. Lagaron, T. Yamamoto, R. Gavara, *Radiation-induced oxygen scavenging activity in EVOH copolymers*, Journal of Applied Polymer Science 105, 2676-2682 (2007).

6. Y.B. Byun, S.I. Hong, K.B. Kim, D.H. Jeon, J.M. KIM, W.S. Whiteside, H.J. Park, *Physical and chemical properties of gamma-irradiated EVOH film*, Radiation Physics and Chemistry 76, 974-981 (2007).

7. P. Budrugeac, T. Zaharescu, M. Marcuta, Gh. Marin, *Accelerated electron effects on EVA based compound*, Journal of Applied Polymer Science 96, 613-617 (2005).

8. W.-A. Zhang, Y.-E. Fang, *Enhancement of radiation-resistant effect in ethylene vinyl acetate copolymers by the formation of ethylene vinyl acetate copolymers/clay nanocomposites,* Journal of Applied Polymer Science 98, 2532-2538 (2005).

9. J.A. Reyes-Labarta, M.M. Olaya and A. Marcilla, *DSC and TGA study of the transitions involved in the thermal treatment of binary mixtures of PE and EVA copolymer with a crosslinking agent*, Polymer 47, 8194-8202 (2006).

10. X. Shi, J. Jin, S. Chen and J. Zhang, *Multiple melting and partial miscibility of ethylene-vinyl acetate copolymer/low density polyethylene blends*, Journal of Applied Polymer Science 113, 2863-2871 (2009).

11. E. Perez, M. Lujan, J. Martinez de Salazar, *Preparation and properties of terpolymers of ethylene, vinyl acetate and vinyl alcohol*, Macromolecular Chemistry and Physics 201, 1323-1328 (2000).

12. M. VarmaNair, B. Wunderlich, *Heat-capacity and other thermodynamic properties of linear macromolecules. 10. Update of the ATHAS 1980 data-bank*, Journal of Physical Chemistry 20, 349-404 (1991).

13. K. Schmidit-Rohr, J. Clauss, H.W. Spiess, *Correlation of Structure, Mobility, and Morphological Information in Heterogeneous Polymer Materials by Two-Dimensional Wideline-Separation NMR Spectroscopy,* Macromolecules 25, 3273-3277 (1991).

14. D. Marks and S. Vega, *A Theory for Cross Polarization NMR of Nonspinning and Spinning Samples*, Journal of Magnetic Resonance, Series A 118, 157-172 (1996).

13. A.A. Parker, J.J. Marcinko, Y.T. Sheih, D.P. Hedrick, W.M. Ritchey, *A Preliminary Correlation Between Macroscopic and Microscopic Polymer Properties – Dynamic Storage Modulus vs. CPMAS NMR Cross Polarization Rates*, Journal of Applied Polymer Science 40, 1717 (1990).

14. J.J. Marcinko, A.A. Parker, P.L. Rinali, W.M. Ritchey, *Application of NMR Cross-Polarization Modulus Correlations to a Series of Polyurethane Elastomer,* Journal of Applied Polymer Science 51, 1777 (1994).

15. R.A. Assink, D.P. Lang, M. Celina, *Condition Monitoring of a Thermally Aged Hydroxy-Terminated Polybutadiene (HTPB)/Isophorone Diisocyanate (IPDI) Elastomer by Nuclear Magnetic Resonance Cross Polarization Recovery Times,* Journal of Applied Polymer Science 81, 453 (2001).

16. C.A. Fyfe, D.H. Brouwer, P. Tekely, *Measurement of NMR Cross-polarization (CP) Rate Constants in the Slow CP Regime: Relevance to structure Determinations of Zeolite-Sorbate and Other Complexes by CP Magic-Angle Spinning NMR,* Journal of Physical Chemistry A. 109, 6178-6192 (2005)

17. C.G. Moth, S.M.D. Castro, M.I.B. Tavare, *Carbon-13 NMR High Resolution and Thermogravimetric Study of CNSL/Compatibility*, Polymer Testing 15, 437-441 (1996).

18. E.R. deAzevedo, W.G. Hu, T.J. Bonagamba, and K. Schmidit-Rohr, *Centerband-Only Detection of Exchange: efficient analysis of Dynamics in Solids by NMR*, Journal of the American Chemical Society 121, 8411-8412 (1999).

19. E.R. deAzevedo, W.G. Hu, T.J. Bonagamba, and K. Schmidit-Rohr, J. *Principles of centerband-only detection of exchange in solid-state nuclear magnetic resonance, and extension to four-time centerband-only detection of exchange,* Journal of Chemical Physics 112, 8988-9001(2000).

20. H.A. Weber, *Determination of phenol in cured parts using HPLC analysis*, LTM 3905-B (03/29/2007).

21. F.J. Pern and A.W. Czanderna, *Characterization of ethylene vinyl acetate (EVA) encapsulant: Effects of thermal processing and weathering degradation on its discoloration*, Solar Energy Materials and Solar Cells 25, 3-23 (1992).